

# Thermal model for analysis of Mars infrared mapping

Hugh H. Kieffer

August 15, 2011

## Contents

<b>1</b>	<b>Introduction</b>	<b>3</b>
1.1	Use for recent missions . . . . .	4
1.2	Some other thermal models used for Mars . . . . .	4
1.3	Notation use here . . . . .	5
<b>2</b>	<b>Physical representation</b>	<b>5</b>
2.1	Planetary Orientation and Orbit . . . . .	5
2.2	Atmosphere . . . . .	5
2.2.1	Delta-Eddington 2-stream . . . . .	5
2.2.2	Twilight . . . . .	6
2.2.3	Atmospheric IR radiation . . . . .	6
2.2.4	Atmospheric temperature . . . . .	6
2.3	Geometry and Starting Conditions . . . . .	7
2.3.1	Geometry . . . . .	7
2.3.2	Starting conditions: Diurnal-average equilibrium . . . . .	8
2.4	CO <sub>2</sub> Frost condensation and Sublimation . . . . .	8
2.4.1	Effective Albedo . . . . .	9
2.4.2	Global and local pressure . . . . .	9
2.5	Boundary conditions . . . . .	9
2.5.1	Level Surface . . . . .	9
2.5.2	Slopes and Conical Holes . . . . .	9
2.5.3	Physical properties, Layering of materials and sub-surface scaling . . . . .	10
2.5.4	Base of model . . . . .	10
2.6	Relation of thermal inertia to particle size . . . . .	10
<b>3</b>	<b>Numerical Methods</b>	<b>10</b>
3.1	Basic Method . . . . .	10
3.2	Finite difference scheme for exponential layer thickness . . . . .	12
3.2.1	Extension to temperature-dependent properties . . . . .	12
3.2.2	Solving the upper boundary condition . . . . .	13
3.2.3	Stability and Binary time expansion . . . . .	13

3.2.4	Starting conditions . . . . .	14
3.2.5	Jump perturbations . . . . .	14
3.2.6	Convergence criteria and parameters . . . . .	14
3.2.7	Prediction to next season . . . . .	15
3.3	Effect of spin-up time, depth and bottom conditions . . . . .	15
3.4	Comparison to other thermal models . . . . .	18
3.4.1	Comparison to Ames GCM . . . . .	18
3.4.2	Comparison to Mellon model . . . . .	20
3.4.3	Comparison to Vasavada model . . . . .	21
<b>4</b>	<b>Effect of T-dependent properties</b>	<b>22</b>
<b>5</b>	<b>Architecture</b>	<b>23</b>
5.1	Main program, KRC . . . . .	24
5.2	Input: TCARD . . . . .	24
5.3	Seasons: TSEAS . . . . .	24
5.4	Latitude calculations: TLATS . . . . .	24
5.5	Diurnal calculations: TDAY . . . . .	25
5.6	Disk Output: TDISK . . . . .	25
5.6.1	Direct Access files . . . . .	25
5.6.2	Packed binary files . . . . .	25
5.7	Commons . . . . .	26
5.8	Options at compilation . . . . .	26
5.9	Print output . . . . .	27
5.9.1	Sample layer table . . . . .	27
<b>6</b>	<b>Use</b>	<b>27</b>
6.1	Linked Runs . . . . .	28
6.2	Routine WHEN2START . . . . .	29
6.3	One-point version: An alternate input . . . . .	29
<b>7</b>	<b>Symbols</b>	<b>31</b>
<b>A</b>	<b>Sample input file for Mars</b>	<b>36</b>
A.1	Example layer table . . . . .	39
<b>B</b>	<b>One-point mode examples</b>	<b>39</b>
B.1	One-point Master file . . . . .	39
B.2	Example One-point Input file . . . . .	40
B.3	One-point sample output . . . . .	41
<b>C</b>	<b>FORTTRAN and C Routines</b>	<b>42</b>
<b>D</b>	<b>Help-List</b>	<b>43</b>

# List of Figures

1	Atmosphere back radiation . . . . .	7
2	Relation between thermal inertia and particle size . . . . .	11
3	One-Point model results . . . . .	16
4	Effect of short or long spinup . . . . .	17
5	Comparison to Ames GCM . . . . .	19
6	Comparison to Mellon models: diurnal . . . . .	20
7	Comparison to Mellon models: seasonal . . . . .	21
8	Comparison to Vasavada model . . . . .	22
9	Effect of temperature-dependent properties . . . . .	23
10	Annual frost mass . . . . .	28

August 15, 2011

## 1 Introduction

This paper describes a numerical model used extensively for computing planetary surface temperatures. The KRC numerical model has evolved over a period of four decades and has been used for a variety of planet, satellite and comet problems, but use has concentrated on Mars. The model uses a one-layer atmosphere but does allow condensation and global pressure variation; the model can output surface kinetic and planetary (nadir view from space) bolometric temperatures, along with a variety of parameters related to subsurface-layer and atmosphere temperatures, seasonal polar cap mass, heat-flow and numerical performance parameters.

The program is designed to compute surface and subsurface temperatures for a global set of latitudes at a full set of seasons, with enough depth to capture the annual thermal wave, and to compute seasonal condensation mass. For historic reasons (it originated in the era of kilo-Hz processors) the code has substantial optimization. It allows sloped surfaces and two zones of different sub-surface materials. There are generalities that allow this code set to be used for any ellipsoid with any spin vector, in any orbit (around any star); with or without an atmosphere (including condensation); this is also the source of some of the complexity.

In response to an oft-asked question, the acronym KRC is simply K for conductivity, R for “rho” ( $\rho$ ) for density, and C for specific heat; the three terms in thermal inertia  $I$ .

KRC uses explicit forward finite differences and is coded in FORTRAN; model development began 1968, and was used to support the Viking mission with a total of 3 cases in an era when computing a single case for 19 latitudes at 40 seasons with a 2-year spinup took an hour on a large university unshared main frame computer<sup>1</sup>. For this reason, the code was highly optimized for speed and uses layer thickness increasing exponentially downward and time steps that increase by factors of two deeper into the subsurface where stability criteria are met. The code is modularized based on time scale and function, and there is extensive use of Commons. The version used for Viking was described briefly in [37]. The KRC model was used in many analyzes of the Viking IRTM data; derivatives were used to study sublimating comets [70] and ring and satellite eclipses [4, 22]. The code has undergone step-wise revision, a major change being a 2002 replacement of a down-going steady IR flux equivalent to fixed fraction of the noon insolation with the atmosphere described here, in which version it has been the basis for analysis of THEMIS and MER Mini-TES results. As of 2009, the code allows temperature-dependent thermal conductivity and specific-heat.

A guide to running KRC is in the file *helplist.tex*; see §D or Supporting material. For THEMIS, a “one-point” capability was included that allows input of a set of points defined by season, latitude, hour and a few major physical parameters; KRC will produce the surface kinetic temperature and planetary brightness temperature for these points; see Section 6.3.

---

<sup>1</sup>An IBM 360-91, at that time the largest (4 Mbyte memory) and fastest (16 \* 1 MIPS) unclassified computer. A rerun of all 3 models on a circa 2009 PC took 5.2 s

## 1.1 Use for recent missions

Although the thermal models for the MGS Thermal Emission Spectrometer (TES) data production were based on the Mellon-Jakosky-Haberle model, which has some heredity from KRC [42, 55], KRC has been used in the analysis of TES data [43, 44]. Extensive comparison of the Mellon model and KRC was done in development of the MGS TES production code.

Determination of thermal inertia using the KRC model has been used in selecting all landing sites on Mars; Pathfinder: [26], MER: [15, 28], Phoenix: [1], MSL: (M. Golombek, personal communication). Post-landing assessment has shown the forecasts of rock abundance to be close [25, 24].

Standard data reduction of the Odyssey Thermal Emission Imaging System (THEMIS) uses the KRC model [13, 14, 57, 65]. This involved generation of a large set of models on a grid of thermal inertia  $I$ , surface albedo  $A$ , elevations and visual dust opacities  $\tau_V$  with output of surface kinetic temperature  $T_s$  and top-of-atmosphere bolometric temperature  $T_b$  at a uniform set of latitudes, Hours  $H$  and seasons. The 7-dimensional model set is interpolated first in season (to correspond to a specific Odyssey orbit), then at the latitude and hour of each observation using the elevation corresponding to the observation longitude; interpolation in opacity and albedo are based on prior or current observations. This leaves  $T_s$  and  $T_b$  as a function of thermal inertia, which may not be monotonic; this relation is interpolated linearly in  $T$ , using either  $T_b$  or opacity-corrected  $T_s$ , and logarithmically in  $I$  to get the thermal inertia. KRC was used in analysis and surface thermal observations by Mini-TES, usually with a similar scheme for  $T_s$  only. [27, 20].

KRC thermal modeling has been used for study of general nature of the Martian surface [5, 6, 7, 18, 3], Chapter 9 in [10]; and detailed sites: [2, 16, 19, 20, 21, 23, 29, 58].

KRC models are the basis for the surface temperature estimate to be used for the black-body emission correction to Mars Reconnaissance Orbiter (MRO) Compact Reconnaissance Imaging Spectrometer for Mars (CRISM) reflection spectra, [41].

KRC [33] and derivatives [51, 52] have been used in study of seasonal slab ice. The capability to model temperatures at the bottom of conical pits was added to study the potential volatile sublimation in freshly exposed trenches to be dug by the Phoenix mission.

In an extreme case, a movie of a thermal day on Mars was made by computing surface temperatures at 0.017 Hour intervals with a "spin-up" of 5 sols at L<sub>s</sub> 90. The measured albedo, thermal inertia and elevation with 0.25 deg resolution in longitude and latitude was used. 1.45 billion instances of KRC "one-point" mode were run on a Dell cluster of 128 CPU's for 48 hours over a weekend. The video can be viewed at [http://mars.asu.edu/phil/l90\\_32\\_full\\_5\\_part\\_movie.mov](http://mars.asu.edu/phil/l90_32_full_5_part_movie.mov) [personal communication from Phil Christensen]

## 1.2 Some other thermal models used for Mars

A finite-difference thermal model used for estimating depth to liquid water stability [17] was made publicly available. A derivative of this model and KRC was used to study ground ice stability [46].

The martian atmosphere has a significant effect on surface temperature, both in the physical temperature of the surface being influenced by the dusty atmosphere's modification of the insolation that reaches the surface, and on the apparent temperature measured remotely by infrared radiometry [30]. Thermal models which treat the atmosphere in detail, such as a dusty radiative/convective column [30] or that include lateral heat transport such in a General Circulation Model (GCM) [31, 8], generally take two to several orders of magnitude longer to compute.

The model used by the U. Colorado group [42] has indirect heritage from KRC and uses a similar subsurface, but has a multi-layer radiative/convective atmosphere; this model was used for TES standard data production.

The goal of the KRC model has been to account for the first-order effects of the atmosphere, while preserving the speed and flexibility to deal with surface effects such as layered materials and sloping surfaces. A complicating factor in treating the atmosphere more fully is that the opacity of Mars's atmosphere can vary considerably in space and time [63]; only GCM's with surface dust interaction model this.

A model similar to KRC in subsurface representation was used largely for Mars' polar studies [49, 47, 48].

### 1.3 Notation use here

Program and routine names are shown as **PROGRAM** [,**N**] , where **N** indicates a major control index. Code variable names are shown **VARIABLE**. Input parameters are shown as **INPUT**. File names are shown as *file*.

For convenience, some physical parameter default values are shown within square brackets at their point of mention and some are listed in Table 7. All units are SI, except the use of days for orbital motion. The sample input file (Appendix A), includes all input parameters. The symbols  $T_s$  and  $T_a$  are used in the text for kinetic temperature of the surface and the one-layer atmosphere.

## 2 Physical representation

### 2.1 Planetary Orientation and Orbit

KRC can accept either fixed heliocentric range and sub-solar latitude, or Keplerian orbital elements and a fixed planet orientation (direction of the spin axis); in both cases, “seasons” are at uniform increments of time. An associated Planetary ORBit program set, **PORB**, main program **porbmn**, accesses files containing the elements for all the planets [61] and a few comets and minor planets ; this program set pre-calculates the orbital elements for any epoch, converts them into rotation matrices for the chosen epoch and creates an ASCII parameter set that is then incorporated into the input file for KRC. For TES and the initial THEMIS modeling, the martian elements were evaluated for epoch 1999; Mars’ spin-axis orientation was based on pre-Viking data, and differs from the current best estimates [60] by about  $0.3^\circ$ . Within KRC, the orbital position of Mars is computed for each “season”, yielding the heliocentric range, the sub-Solar latitude, and the seasonal indicator  $L_s$ .

Planetary orientations have been updated to [60] and mean elements have been updated to [59].

For Mars, the maximum error in ecliptic longitude is under 30 arc-sec, corresponding to about 1/60 of a sols’ motion, which is negligible compared to the assumption of ignoring Martian longitude.

### 2.2 Atmosphere

KRC uses a one-layer atmosphere that is gray in the solar and thermal wavelength ranges. Radiative exchange with the Sun, space and the surface determines the atmosphere energy balance and its temperature variation. The columnar mass (and the surface pressure) can vary with season and surface elevation. A uniformly-mixed dust loading is allowed to modify the visual and thermal opacity. Direct and diffuse illumination are computed using a double-precision 2-stream Delta-Eddington model, with single scattering albedo  $\varpi$  and Henyey-Greenstein asymmetry parameter  $G_H$ . The thermal opacity is a constant factor  $C_2$  times the visual opacity. An option allows an extension of twilight past the geometric terminator.

The current local solar-wavelength atmospheric opacity of dust,  $\tau$ , can vary with atmospheric pressure:  $\tau = \tau_0 \cdot P/P_0$

#### 2.2.1 Delta-Eddington 2-stream

A Delta-Eddington model is used for atmosphere scattering and fluxes (**deding2.f**); output parameters are normalized to unit solar irradiance along the incident direction at the top of atmosphere; so they must be multiplied by  $S_M$ , the solar irradiance at the current heliocentric range,  $S_M$  to get flux.

Scattering parameters used are the aerosol single scattering albedo  $\varpi$  and the scattering asymmetry parameter [32]; both are input constants. The computed values include:

Planetary (atmosphere plus surface system) albedo: **BOND**

Direct beam at the bottom, includes both collimated and aureole:  $F_{\parallel} = \text{COLL}$

Diffuse irradiances:  $I_{i,j}$

$i$ : 1 = isotropic, 2 = asymmetric

$j$ : 1 = at top of atmosphere, 2 = at bottom of atmosphere

The net diffuse flux is  $F_{\ominus} = \pi[I_{1j} \pm \frac{2}{3}I_{2j}]$  where + is down,  $F_{\ominus}^{\downarrow}$ ; - is up,  $F_{\ominus}^{\uparrow}$  . [62, eq. 8]

The total down-going solar flux at the bottom of the atmosphere is

$$S'_t = S_M \left( \mu_0 F_{\parallel} + F_{\ominus}^{\downarrow} \right) \quad (1)$$

where  $\mu_0 \equiv \cos i_0$  and the diffuse component is  $F_{\ominus}^{\downarrow} = \pi \left( I_{1,2} + \frac{2}{3} I_{2,2} \right)$ .

Solar heating of the atmosphere, by conservation of energy, is

$$H_V = S_M \left( \mu_0 - F_{\ominus}^{\uparrow}(0) - (1 - A_s) \left[ \mu_0 F_{\parallel} + F_{\ominus}^{\downarrow}(\tau) \right] \right). \quad (2)$$

### 2.2.2 Twilight

Twilight is allowed to account for having a turbid atmosphere. It is implemented as having the diffuse downward illumination depend upon an incidence angle scaled to go to  $90^\circ$  when the Sun is TWILI below the geometric horizon.

Because of the twilight extension, there can be a small negative energy balance near twilight. Physically, this is lateral scattering and does not strictly fit a one-layer model. There is no solar heating of the atmosphere during twilight.

### 2.2.3 Atmospheric IR radiation

The IR opacity is approximated as  $\tau_R = P/P_0 \cdot (C_1 + C_2\tau)$  where  $C_1$  represents the opacity of the “clear” atmosphere, primarily due to the  $15\mu\text{m}$   $\text{CO}_2$  band, and  $C_2$  is the IR/visual opacity ratio for dust.

The fractional thermal transmission of the atmosphere at zenith is roughly  $e^{-\tau_R}$ . The fractional absorption is  $\beta \equiv 1 - e^{-\tau_R}$ .

The fractional transmission of planetary (thermal) radiation in a hemisphere is:

$$e^{-\tau_e} \equiv \int_0^{90} e^{-\tau/\cos\theta} \cos\theta \sin\theta \, d\theta \quad (3)$$

Numerical integration shows that the effective hemispheric opacity is, within about 0.05 in the factor,

$$\tau_e \sim [1.0 < (1.50307 - 0.121687 * \ln \tau_R) < 2.0] \tau_R; \quad (4)$$

this is used in the effective absorption  $\beta_e \equiv 1 - e^{-\tau_e}$ .

The hemispheric downward (and upward) emission from a gray slab atmosphere is:  $R_{\downarrow} = \sigma T_a^4 \beta_e$ . The IR heating of the atmosphere is:

$$H_R = \epsilon \sigma T_s^4 (1 - e^{-\tau_e}) - 2R_{\downarrow} = \sigma \beta_e (\epsilon T_s^4 - 2T_a^4) \quad (5)$$

To estimate the back-radiation from a clear atmosphere, a synthetic transmission spectrum of the Mars atmosphere with a nominal amount of water vapor (provided by David Crisp) was multiplied by blackbody spectra for a range of temperatures to determine the fraction of radiation blocked, see Figure 1. A coefficient of  $C_1 = 0.11 \pm 0.004$  covers the range 187K to 293K.

### 2.2.4 Atmospheric temperature

The atmospheric temperature is assumed to follow radiative energy conservation:

$$\frac{\partial T_a}{\partial t} = \frac{H_R + H_V}{c_p M_a} \quad (6)$$

where  $M_a = P/G$  is the mass of the atmosphere and  $c_p$  is its specific heat at constant pressure.

Because the atmospheric temperature variation has significant time lag relative to the surface, one can use the surface temperature from the prior time step (typically 1/384 of a sol) with little error.

If the computed atmospheric temperature at midnight drops below the  $\text{CO}_2$  saturation temperature for one scale height above the local surface, it is bounded at this value and the excess energy loss is converted to snow. If there is

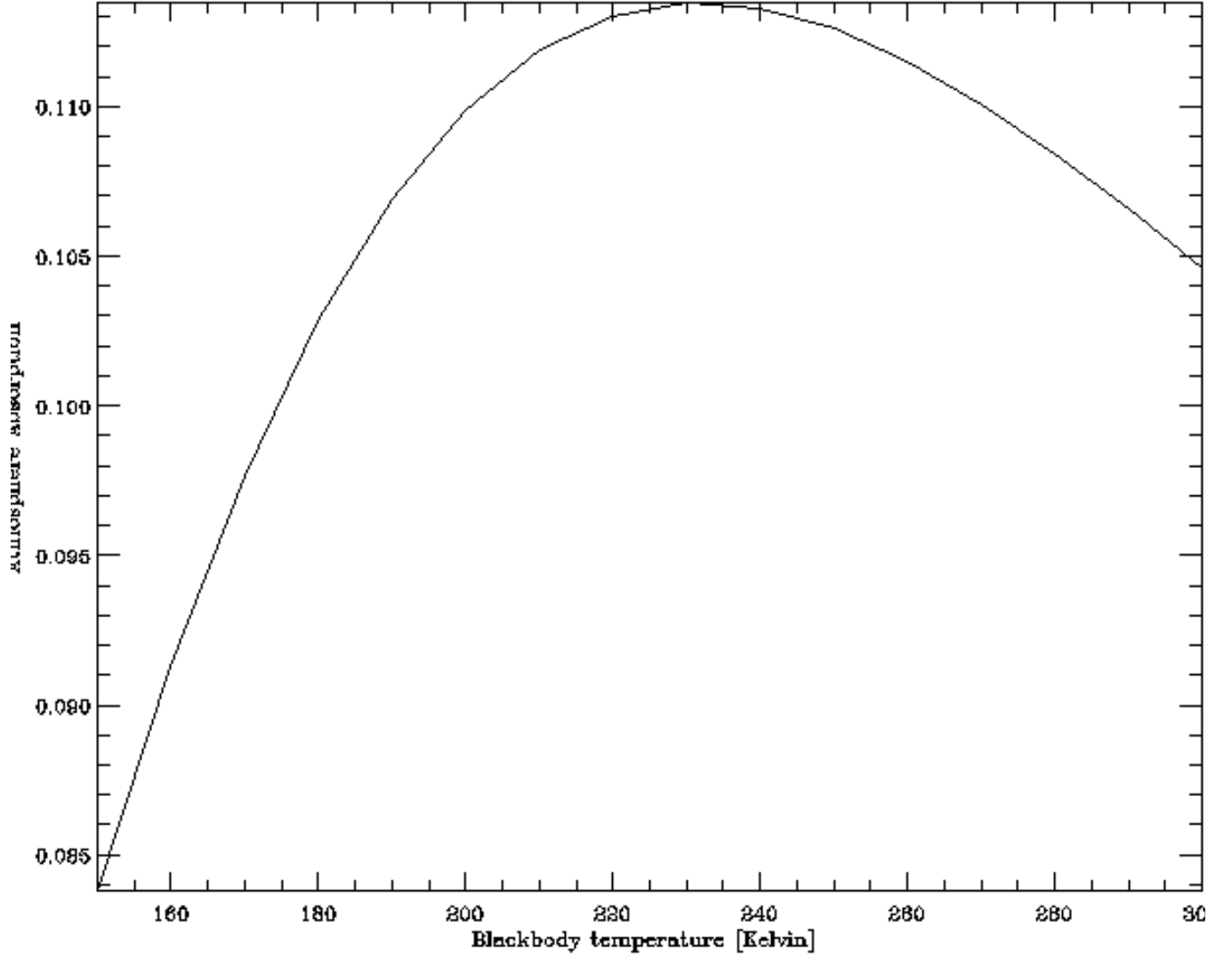


Figure 1: Blocking of thermal radiation by a dust-free Mars atmosphere. Ordinate is the fraction of blackbody radiation absorbed by a nominal atmosphere of 700 Pa CO<sub>2</sub> with a nominal amount of water vapor. Abscissa is the blackbody temperature.

frost on the ground, this snow mass is added to the frost; otherwise it is ignored in the heat budget, which strictly does not conserve energy.

$$\Delta M = \Delta T c_p M_a / L \quad (7)$$

The nadir planetary temperature is given by

$$\sigma T_P^4 = \epsilon \sigma T_S^4 (e^{-\tau_R}) + \sigma T_a^4 (1 - e^{-\tau_R}) \implies T_P = [\epsilon(1 - \beta)T_S^4 + \beta T_a^4]^{1/4} \quad (8)$$

## 2.3 Geometry and Starting Conditions

### 2.3.1 Geometry

The diurnal variation of insolation onto the surface at the bottom of the atmosphere is computed for the current season and latitude. The incidence angle from zenith onto the horizontal plane ( $i_0$ ) or sloped surface is computed by:

$$\cos i = \sin \delta \sin (\theta + s_N) - \cos \delta \cos (\theta + s_N) \cos (\phi + s_E) \quad (9)$$

where

- $\delta$  = the solar declination,
- $\theta$  = latitude,
- $\phi$  = hour angle from midnight,
- $s_N$  = north component of surface slope,
- $s_E$  = east component of surface slope,

Direct (collimated) insolation is computed for the local surface, which may be sloped in any direction and has incidence angle  $i_2$ ;

Direct insolation is zero when either  $i_0$  or  $i_2$  is  $> 90^\circ$ . Diffuse illumination is based on  $i_0$ , with the optional extension into twilight (see Section 2.2.2). For a sloped surface, the solid angle of skylight is reduced and light reflected off the regional surface (presumed Lambert and of the same albedo) is added; the Delta-Eddington downward diffuse radiance is multiplied by  $\text{DIFAC} = 1 - \alpha + \alpha A$ , where  $\alpha = (1 - \cos i_2) / 2$  is the fraction of the upper hemisphere obscured by ground. For the small flat bottom of conical pits,  $\alpha = \sin^2 (\frac{\pi}{2} - s)$  where  $s$  is the slope of the pit wall from horizontal.

If a sloping surface (or pit) is used, the regional horizontal surface (or pit wall) is assumed to be at the same temperature, which becomes a poor approximation for steep slopes.

The incident flux at the top of atmosphere is:  $I = S_M \cos i_0$ , where  $S_M \equiv \frac{S_o}{U^2}$ ,  $S_o$  is the solar constant and  $U$  is heliocentric range of Mars in Astronomical Units.

### 2.3.2 Starting conditions: Diurnal-average equilibrium

For the first season, the atmosphere temperature is set based on the equilibrium for no net heating of the atmosphere or surface, using the diurnal average of insolation (see Eq. 2 and Eq. 5):

$$\langle H_V \rangle + \langle H_R \rangle = 0 \quad (10)$$

Surface radiation balance, from Eq. 13 for a flat surface with no net sub-surface heat flow:

$$\epsilon \sigma \langle T_s^4 \rangle = (1 - A) \langle S'_{(t)} \rangle + \epsilon \sigma \beta_e \langle T_a^4 \rangle \quad (11)$$

Expansion of  $\langle H_R \rangle$  using Eq. 5 and substitution into Eq. 11, yields ;

$$\langle T_a^4 \rangle = \frac{\langle H_V \rangle / \beta_e + (1 - A) \langle S'_{(t)} \rangle}{\sigma(2 - \epsilon \beta_e)} \quad (12)$$

Substitute into Eq. 11 to get  $\langle T_s \rangle$ . For computational simplicity, the average top-of-atmosphere insolation is used as an approximation for  $\langle S'_{(t)} \rangle$ ; this slightly over-estimates the temperature of the atmosphere at the start of the first season.

The planetary heating values are based on the average surface temperatures from the prior season; this is similar to allowing some long-term lag in total atmospheric temperature response.

## 2.4 CO<sub>2</sub> Frost condensation and Sublimation

The local frost condensation temperature  $\text{TFNOW}$  may be either fixed at an input value  $\text{TFROST}$ , or derived from the local surface partial pressure at the current season.

The relation between condensation/sublimation temperature and partial pressure is taken to be the Clausius-Clapeyron relation:  $\ln P_c = a - b/T$ , in **CO2PT** with  $a=27.9546$  [Pascal] and  $b=3182.48$  [1/Kelvin], derived from [36] page 959.

If frost is present,  $E = W \cdot \Delta t$  energy is used to modify the amount of frost;  $\Delta M = -E/L$ , where  $L$  is the latent heat of sublimation. The frost albedo may depend upon insolation, and there may be an exponential attenuation of the underlying ground albedo; see §2.4.1. The amount of frost at each latitude is carried (asymptotic prediction) to the next season.



### 2.4.1 Effective Albedo

A thick frost deposit can have a constant albedo, or be linearly dependent upon the insolation as described by [45, 38]. It should be noted that it is now known that regions of the seasonal caps can have virtually constant low albedo, [38, 66].

As the seasonal frost thins, the effective albedo of the surface can continuously approach that of underlying soil.  $A = A_f + (A_s - A_f)e^{-M/M_e}$  where  $M_e$  is the frost required,  $\text{kg m}^{-2}$ , for unity scattering attenuation.

### 2.4.2 Global and local pressure

The total amount of atmosphere is set by the annual mean surface pressure at the reference elevation,  $P_0$ , input as PTOTAL.

The current global pressure  $P_g = \text{PZREF}$ , can be any of the following:

- 1) constant at  $P_0$
- 2)  $P_0$  times the normalized Viking Lander pressure curve computed in **VLPRES** [64]
- 3) Based on depletion of atmospheric  $\text{CO}_2$  by growth of frost caps;  $P_0$  minus the total frost mass at the end of the prior season. Requires that the number of latitudes  $\text{NLAT} > 8$ .

The initial partial pressure of  $\text{CO}_2$  at zero elevation is  $P_{c0} = P_0 \cdot (1 - \text{non-condensing fraction}) = \text{PCO2M}$ . The current  $\text{CO}_2$  partial pressure at zero elevation is  $P_{cg} = P_{c0} + (P_g - P_0) = \text{PCO2G}$ .

Both the current local total pressure and  $\text{CO}_2$  partial pressure scale with surface elevation and scale height:  $P \propto e^{-z/\mathcal{H}}$ . The scale height is:  $\mathcal{H} = T_a \mathcal{R} / \mathcal{M}G$ ; where  $T_a$  is the mean atmospheric temperature over the prior day (or season),  $\mathcal{R}$  is the universal gas constant,  $\mathcal{M}$  is the mean molecular weight of the atmosphere (43.5), and  $G$  is the martian gravity.

Local current dust opacity scales with local total pressure:  $\tau = \tau_0 \cdot P/P_0$ . The atmospheric saturation temperature is evaluated at one scale height above the local surface; if  $T_a$  would fall below this, condensation is assumed to take place to provide the energy required to prevent this, and the snow is added to the surface frost budget.

## 2.5 Boundary conditions

### 2.5.1 Level Surface

The surface condition for a frost-free level surface is :

$$W = (1 - A)S'_{(t)} + \Omega \epsilon R_{\downarrow} + \frac{k}{X_2}(T_2 - T) - \Omega \epsilon \sigma T^4 \quad (13)$$

where  $W$  is the heat flow into the surface,  $A$  is the current surface albedo,  $S'_{(t)}$  is the total solar radiation onto the surface as in Eq. 1,  $R_{\downarrow}$  is the down-welling thermal radiation (assumed isotropic),  $T$  is the kinetic temperature of the surface,  $k$  is the thermal conductivity of the top layer,  $X_2$  is the depth to the center of the first soil layer, and  $T_2$  the temperature there.  $\Omega$  is the visible fraction of the sky; for level surfaces,  $\Omega = 1$ .  $\epsilon$  is the surface emissivity and  $\sigma$  the Stefan-Boltzman constant. In the absence of frost, the boundary condition is satisfied when  $W=0$ . Most constant terms are precomputed, see Table 7.

When frost is present, the values in Eq. 13 are replaced with  $\epsilon_F$ ,  $A_F$ , and  $T_F$ , where subscript  $F$  indicates the frost values, and no iteration is done; leaving  $W$  as a non-zero quantity to change the frost amount. See Section 2.4.

### 2.5.2 Slopes and Conical Holes

The surface condition for a planar sloped surface or a conical pit with a small flat bottom modifies the interaction with the radiation field. This is simplified by using the crude approximation that the surfaces visible to the point of computation are at the same temperature and have the same brightness where illuminated. Then

$$S'_t = S_M \left[ F_{\parallel} \cos i_2 + \Omega F_{\odot}^{\downarrow} + \alpha A (G_1 F_{\parallel} + \Omega F_{\odot}^{\downarrow}) \right] \quad (14)$$

$F_{\parallel}$  is the collimated beam in the Delta-Eddington model and  $F_{\odot}^{\downarrow}$  is the down-going diffuse beam.  $G_1$  is the fraction of the visible surrounding surface which is illuminated. Within the brackets in Eq. 14,

the first term is the direct collimated beam, DIRECT

the second is the diffuse skylight directly onto the target surface, DIFFUSE

the third term is light that has scattered once off the surrounding surface, BOUNCE

For a sloped surface,  $G_1$  is taken as unity. As a first approximation, for pits  $G_1 = (90 - i)/s < 1$  where  $s$  is the slope of the pit walls. For a flat-bottomed pit,  $i_2 = i$  when the sun is above the pit slope, and  $\cos i_2 = 0$  when below.

### 2.5.3 Physical properties, Layering of materials and sub-surface scaling

All physical properties are specified by parameters in the input file. Nominal planetary parameters for Mars are the mean solar day, 1.0275 days, and the surface gravity,  $3.727 \text{ m s}^{-2}$ . Properties of the upper-layer material are specified by the specific heat  $C_p$  [J/(kg K)], density  $\rho$  [kg/m<sup>3</sup>] and thermal inertia  $I$  [J m<sup>-2</sup> s<sup>-1/2</sup> K<sup>-1</sup>], which in turn sets the conductivity  $k$  [W/(K m)]

Beginning with layer IC, all lower layers can have their conductivity, density and volume specific heat reset to COND2, DENS2, and SPHT2 respectively. If LOCAL is set true, then the physical thickness of these layers scales with the local thermal diffusivity; otherwise, the geometric increase of physical layer thickness continues downward unaltered.

### 2.5.4 Base of model

Normally, the base of the model is treated as insulating. However, there are also options for it to be held at a fixed temperature, which is useful to model subsurface H<sub>2</sub>O ice.

## 2.6 Relation of thermal inertia to particle size

The relation of  $I$  to particle diameter is based on laboratory measurements,[53]; the specific relation shown in Figure 2 is for P=600 Pascal, density=1600 kg/m<sup>3</sup> and specific heat=625.

A histogram was made of the Thermal inertia determined from TES global map data, [54], although this used a different thermal model. The  $I$  source data are available at <http://lasp.colorado.edu/inertia/2007/>; these data were weighted by area. Most areas are in  $I$  range of 100:500; values above about 200 are increasingly affected by a rock population or real bedrock, which has  $I \sim 2000$ .

## 3 Numerical Methods

The addition of temperature-dependent conductivity is treated as a variation to the constant-conductivity version.

### 3.1 Basic Method

The user inputs the thermal inertia  $I$ , the bulk density  $\rho$ , and the specific heat of the material  $C_p$ . Thermal conductivity  $k$  is computed from  $I^2/(\rho C_p)$ . The thermal diffusivity is  $\kappa = \frac{k}{\rho C_p}$ . While  $k$ ,  $\rho$ , and  $C_p$  do not independently influence the surface temperature for a homogeneous material, they set the spatial scale of the subsurface results;  $\text{SCALE} = \sqrt{\kappa \frac{P}{\pi}}$ , where  $P$  is the diurnal period in seconds.

KRC uses layers that increase geometrically in thickness  $B_i =$  by a factor  $R = \text{RLAY}$ . In order to simplify the innermost code loops, KRC places the radiating surface between the first and second model layers; the top (virtual) layer has physical thickness of  $\text{FLAY} * \text{SCALE}$  meter. The layer index  $i$ , increases downward. Layer 1 is above the physical surface; below, subscript +(-) is shorthand for  $i + (-)1$ ;  $i+.5$  is the lower boundary of the layer.

Basic differential equation of heat flow is :

$$\frac{\partial T}{\partial t} = \frac{-1}{\rho C_p} \frac{\partial}{\partial z} \left( -k \frac{\partial T}{\partial z} \right) = \frac{k}{\rho C_p} \frac{\partial^2 T}{\partial z^2} \quad (15)$$

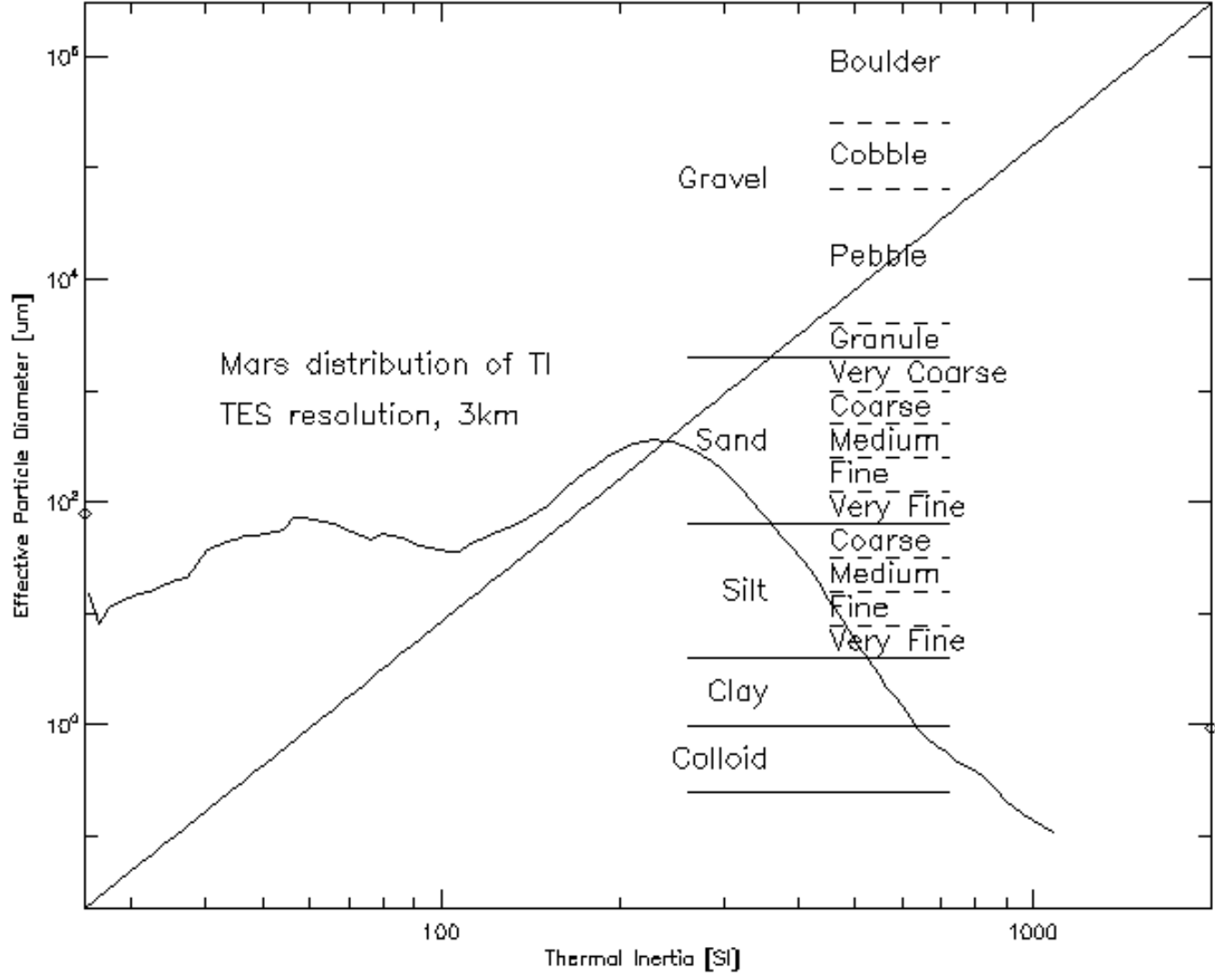


Figure 2: Nominal relation between thermal inertia and effective particle size, shown as the nearly straight line; specific conditions are  $P=600$  Pascal, density= $1600$  kg/m<sup>3</sup> and specific heat= $625$ . The size designations are standard Wentworth scale. The areal distribution of thermal inertia on Mars between latitudes  $65S$  and  $70N$  is shown as the jagged line, derived from mapping using TES night-time data [55]; note the log scale, vertical position arbitrary. The bimodal distribution peaks at  $60$  and  $200$  (dominant), corresponding to the low limit for clay (particle diameter  $1 \mu\text{m}$ ) and medium sand (particle diameter  $0.5$  to  $1$  mm). Values above about  $500$  are increasingly affected by a rock population or real bedrock. The small diamonds at the left and right limits indicate the sum of all values outside the plotted abundance range.

where  $t$  = time,  $T$  = temperature and  $z$  is the vertical coordinate.

Expressed for numerical calculations:

$$\frac{\Delta T_i}{\Delta t} = -\frac{H_{i+0.5} - H_{i-0.5}}{B_i \rho_i C_{p_i}} \quad (16)$$

where  $B_i$  = is the layer thickness and  $H$  = heat flow at the boundary.

Use steady-state relations to find heat flow at interface between two layers:  $H = -k\nabla T$

$$H_{i+0.5} = -\frac{T' - T_i}{B_i/2} k_i \quad \text{or} \quad T' - T_i = -\frac{H_{i+0.5} B_i}{2k_i} \quad (17)$$

where  $T'$  is the temperature at the interface.

$$\text{Similarly } T_{i+1} - T' = -\frac{H_{i+.5}B_{i+1}}{2k_{i+1}}$$

$$\text{Thus } T_{i+1} - T_i = -\frac{H_{i+.5}}{2} \left( \frac{B_i}{k_i} + \frac{B_{i+1}}{k_{i+1}} \right)$$

$$\text{or } H_{i+.5} = -\frac{2(T_{i+1} - T_i)}{\frac{B_i}{k_i} + \frac{B_{i+1}}{k_{i+1}}} \quad \text{Similarly} \quad H_{-.5} = -2\frac{T - T_-}{\frac{B}{k} + \frac{B_-}{k_-}}$$

For uniform layer thickness in uniform material, the standard form of explicit forward difference is

$$\frac{\Delta T_i}{\Delta t} = \frac{\kappa}{B^2} [T_+ - 2T_i + T_-].$$

### 3.2 Finite difference scheme for exponential layer thickness

The depth parameter is scaled to the diurnal thermal skin-depth. For variable layer thickness:

$$\frac{\Delta T_i}{\Delta t_i} = \frac{2}{B_i \rho_i C_{p_i}} \left[ \frac{T_+ - T_i}{\frac{B_i}{k_i} + \frac{B_+}{k_+}} - \frac{T_i - T_-}{\frac{B_i}{k_i} + \frac{B_-}{k_-}} \right] \quad (18)$$

Formulate as

$$\Delta T_i = F_{1_i} [T_+ + F_{2_i} T_i + F_{3_i} T_-] \quad (19)$$

Define intermediate constants for each layer:

$$F_{1_i} = \frac{2\Delta t_i}{B_i \rho_i C_{p_i}} \cdot \frac{1}{\frac{B_i}{k_i} + \frac{B_+}{k_+}} \equiv \frac{2\Delta t_i}{\rho_i C_{p_i} B_i^2} \cdot \frac{k_i}{1 + \frac{B_+}{B_i} \frac{k_i}{k_+}} \quad (20)$$

and

$$F_{3_i} = \left( \frac{B_i}{k_i} + \frac{B_+}{k_+} \right) \cdot \frac{1}{\frac{B_i}{k_i} + \frac{B_-}{k_-}} \equiv \frac{1 + \frac{B_+}{B_i} \frac{k_i}{k_+}}{1 + \frac{B_-}{B_i} \frac{k_i}{k_-}} \quad (21)$$

and

$$F_{2_i} = -(1 + F_{3_i}) \quad (22)$$

Then the inner-most loop, one time-step for one layer, is Eq. 19 followed by

$$T_i = T_i + \Delta T_i \quad (23)$$

The input parameter FLAY specifies the thickness of the top “virtual” layer is dimensionless units (in which the diurnal skin-depth is 1.0), so that the scaled thickness of the uppermost layer in the soil is FLAY\*RLAY, and the physical depth of its center in meters is 0.5\*FLAY\*RLAY\*SCALE. Normally (LP2 set true) a table of layer thickness, depth, (both scaled and in meters), overlying mass, and numerical convergence factor is printed out at the start of a run.

#### 3.2.1 Extension to temperature-dependent properties

Temperature-dependent properties must be evaluated at each layer and time-step.

Because conductivities and layer thicknesses appear largely as ratios, KRC calculates these as infrequently as possible.  $k(T)$  is implemented as a third-degree polynomial; expecting that the linear and quadratic term will cover the variation in gas conductivity and the cubic term the radiation effect. To minimize roundoff problems, the polynomial uses a scaled independent variable  $T' = (T - T_{off}) * T_{mul} = (T - 220.) * 0.01$ . Because KRC allows two materials, this requires a total of 8 coefficients.[Implemented 2008 Feb]

Specific heat increases with temperature for geologic materials and martian conditions. Theoretical models range from the classic model of Debye to the comprehensive formulation of S.W. Kieffer [39]. There are several few-term empirical relations, e.g.  $\frac{A}{B+T}$ ,  $\left(\frac{T}{T_c}\right)^\beta$ , polynomial in  $\frac{T-T_c}{T_c}$  [40],  $c_1 - c_2/\sqrt{T} - c_3T^{-2} + c_4T^{-3}$  where all coefficients are positive [11], and others in [69]. However, it was found that over the full range of martian temperatures a cubic polynomial would fit geologic materials with error  $< 1\%$ . A temperature-scaled polynomial of the same form as for thermal conductivity has been implemented [2010 Feb].

An informal description of the literature search on thermal properties and the development of code to generate the cubic-polynomial coefficients is contained in [35]. A separate study of the theoretical variation of the effective thermal conductivity of particulate materials as a function of grain-size, cementing and temperature, inspired by the early versions of the numerical modeling of [52, 50] was done [34]. Both of these are available as supplementary material.

The layer setup described in the prior section remains based on the values of the physical properties at a reference temperature, chosen to be 220 K, which is the approximate midpoint of the full range of surface temperatures on Mars.

Compute once per run:  $F_{C_i} = 2\Delta t_i / (\rho_i B_i^2)$  and  $F_{B_i} = B_+ / B_i$

Compute once per time step:  $F_{k_i} = k_i / k_+$

Then Equations 20 and 22 become

$$F_{1_i} = F_{C_i} \cdot \frac{k_i / C_P(T)}{1 + F_{B_i} F_{k_i}} \quad (24)$$

and

$$F_{3_i} = \frac{1 + F_{B_i} F_{k_i}}{1 + 1 / (F_{k_-} F_{B_-})}. \quad (25)$$

Eq. 22 remains the same, but must be evaluated for every layer and time-step.

### 3.2.2 Solving the upper boundary condition

When there is no surface frost, the net energy into the upper boundary must be zero. From Eq. 13, find

$$\frac{\partial W}{\partial T} = -k / X_2 - 4\Omega\epsilon\sigma T^3 \quad (26)$$

Note that this assumes that the temperature gradient in top half of layer 2 is linear. If KofT, then  $k$  is approximated as that of the top material layer at the end of the prior time-step.

The surface kinetic temperature for a balanced boundary condition, Eq. 13, is iterated with Newton convergence until the change in  $T$ ,  $\delta \equiv \frac{W}{\partial W / \partial T}$ , is  $< \text{GGT}$

If  $|\delta| / T > 0.8$ , it is assumed that the model has gone unstable and it is terminated.

if  $|\delta| / T > 0.1$ , then  $\delta$  is reduced by 70% before the next iteration to improve stability

If frost is present, the unbalanced energy  $W$  is applied to condensation or sublimation.

After determining the surface temperature, the virtual layer ( $i = 1$ ) temperature is set to yield the proper heat flow between the surface and the top physical layer ( $i = 2$ );

$$T_1 = T' - (T_2 - T') \frac{B_1 \kappa_2}{B_2 \kappa_1} \quad \text{OR} \quad T_1 = T_2 - (1 + 1/\text{RLAY}') (T_2 - T') \quad (27)$$

where the diffusivity of the virtual layer can be treated as identical to the top physical layer.

### 3.2.3 Stability and Binary time expansion

The classic convergence stability criterion is  $\frac{\Delta t}{(\Delta Z)^2} \kappa < \frac{1}{2}$ , equivalent to  $B^2 > 2\Delta t \kappa$ . A convergence safety factor is defined as  $B_i / \sqrt{2\Delta t_i \cdot \kappa_i}$ . The code was found to be numerically unstable if this factor is less than about 0.8. The routine will stop with an error message if the safety factor is anywhere less than one. As the layer thickness increases with depth, the routine will repeatedly double the time interval if all the following conditions are met:

The safety factor is larger than 2

The layer is at least the 3rd down  
 The remaining time intervals are divisible by 2  
 No more than MAXBOT time doublings will be done

To handle potential large jumps in diffusivity that are allowed between two materials, an initial calculation of the safety factor for the upper layer of the lower material is made without time-doubling. If this does not meet the input convergence factor CONVF, then the thickness of this and all lower layers is increased to be stable with this safety factor. If the thickness of this key layer is overly conservative, then the number of allowed time-doubling in the upper materials is set accordingly.

The numerous input parameters that control the time-depth grid and convergence are based upon extensive testing done during the code development.

### 3.2.4 Starting conditions

For the first season, the model starts at 18 Hours with the surface temperature normally set to the equilibrium surface temperature of a perfect conductor as calculated in Eq. 11. The bottom temperature is also normally set to this value. The input parameter IB allows the option of setting the initial bottom temperature to TDEEP or also the surface temperature to this value; the latter case is useful for studying details of the disappearance of seasonal frost.

Once the top and bottom temperatures are set, all intermediate layer temperatures are set by linear interpolation with depth. The initial atmosphere temperature is always set to the equilibrium values using Eq. 12.

### 3.2.5 Jump perturbations

A logical flag LRESET is normally false. It is set True on day NRSET or later of the first season if the lower boundary is adiabatic, but never on the last day of calculation in a season or if the lower boundary temperature is fixed.

On a day when LRESET is true, the summation for average layer temperatures is restarted. At the end of that day, all layer temperatures are offset by  $\langle T_s \rangle - \langle T_i \rangle$  so as to yield no net heat flow.

There is an option to instead perturb temperatures based on a linear plus fractional quadratic function of depth between the diurnal average surface and diurnal average bottom temperatures: if DRSET is not zero, then the layer temperature offsets are, using  $x = z_i/z_n$  where  $n$  is the bottom layer:

$$\Delta T_i = (\langle T_s \rangle - \langle T_n \rangle) (x + \text{DRSET} \cdot x(1 - x))$$

### 3.2.6 Convergence criteria and parameters

At each time step, if there is not frost, the surface boundary equation is iterated until the change in surface temperature is less than GGT.

The test for continuing full computations each day into a season is based upon  $\Delta_T$ , defined as the RMS change of layer temperatures at midnight, including the virtual layer, from midnight the prior day; this is stored at the end of each day in DTMJ

The test for making the next day the last is: either the temperature change over the last two days is nearly constant, or the temperature change is small; i.e.:

$$\left| 1 - \frac{\Delta_{T,j}}{\Delta_{T,j-1}} \right| \leq \text{DDT} \quad \text{or} \quad \Delta_T \leq \text{DTMAX}$$

where  $\Delta_{T,j-1}$  is forced to be at least  $10^{-6}$ . Normally, DDT = 0.002, GGT = 0.1 and DTMAX = 0.1

After computation of the last day, there is a final check that convergence has continued: the temperature change has decreased or it is still small; i.e.:

$$\Delta_T \leq \Delta_{T,j-1} \quad \text{or} \quad \Delta_T \leq \text{DTMAX}$$

If these tests fail, and there are days left in the season, then daily calculations are resumed.

### 3.2.7 Prediction to next season

Calculations run from midnight to midnight. When convergence has been reached, commonly in fewer days than separate seasons, the results at the last 3 midnights,  $y_1, y_2, y_3$ , are used to forecast asymptotically the model result at the end of the season,  $y = b_0 + b_1 r^x$  where  $x$  is the number of sols remaining in the season. Normally, this will use a fit over the last 3 midnights; for convenience reformulated as

$$y = y_3 + c_1((1. - r^x) \tag{28}$$

where  $r = \frac{y_3 - y_2}{y_2 - y_1}$  is the ratio of the last two changes, and  $c_1 = \frac{y_3 - y_2}{1/r - 1}$ . If the fit is not asymptotic (e.g., if  $r \geq 1$ ), or if the forecast distance (from the last computed midnight) is less than 0.9 sols, the routine will do a linear prediction using the most recent two points. In addition, lower and upper limits can be specified, e.g., to keep a temperature from falling below a frost point.

### 3.3 Effect of spin-up time, depth and bottom conditions

The default atmosphere has a time constant of a few sols, so that its initial state has little effect for runs a modest factor longer than this; e.g., the default onePoint mode, which has a 15 sol effective spinup.

KRC has three lower boundary condition options; the first is the default.

**IB=0** All layers start at the equilibrium temperature for the starting season. The boundary is insulating and after a few sols all layers "jumped" to the same average as the surface.

**IB=1** Top starts at the equilibrium temperature and the bottom at TDEEP, intermediate layers linear with depth. Bottom boundary insulating and no jump is done.

**IB=2** All layers start at TDEEP and the lower boundary is held at this value. Useful for spring frost recession details. Effect compared to IB=1 diminishes with time-constant of the model total thickness.

Effects related to bottom conditions generally are largest predawn, and about  $\frac{1}{2}$  that amount at midday; this is shown in Figure 3 which shows the difference in  $T_s$  of a 4 year spinup relative to the OnePoint mode; both models run with IB=0.

For three latitudes (VL-1, equator and 25 S) at  $L_s = 100^\circ$ , short and long spin-up time were tried; 20 sols and  $3\frac{1}{4}$  Mars years, with three sets of lower boundary conditions and 10, 13, 16, 19 and 29 layers, corresponding to total model thicknesses of 4.5, 8.5, 15.6, 27.7 and 177 diurnal skin-depths; the last two correspond to 1.1 and 6.8 annual skin-depths. TDEEP was set to 180, intentionally about 20 K below the annual average of  $T_s$ ; with this large initial offset there is some residual effect for deep models with IB=2 even after 4 years. The results are shown in Figure 4. The seasonal excursions at 25 S, with an zenith noon Sun near perihelion, are about triple those at VL-1.

The effect of deep-layer memory is largest for the ground surface at night, when other heat sources are minimum. The effect near midday and in the atmosphere at all hours is less, both by roughly a factor of 0.6.

If realization of annual effects is desired, a reasonable choice is IB=0, with a total thickness of about 25 diurnal skin-depths (1 annual skin-depth), starting near an equinox, and a spinup of about 2 years.

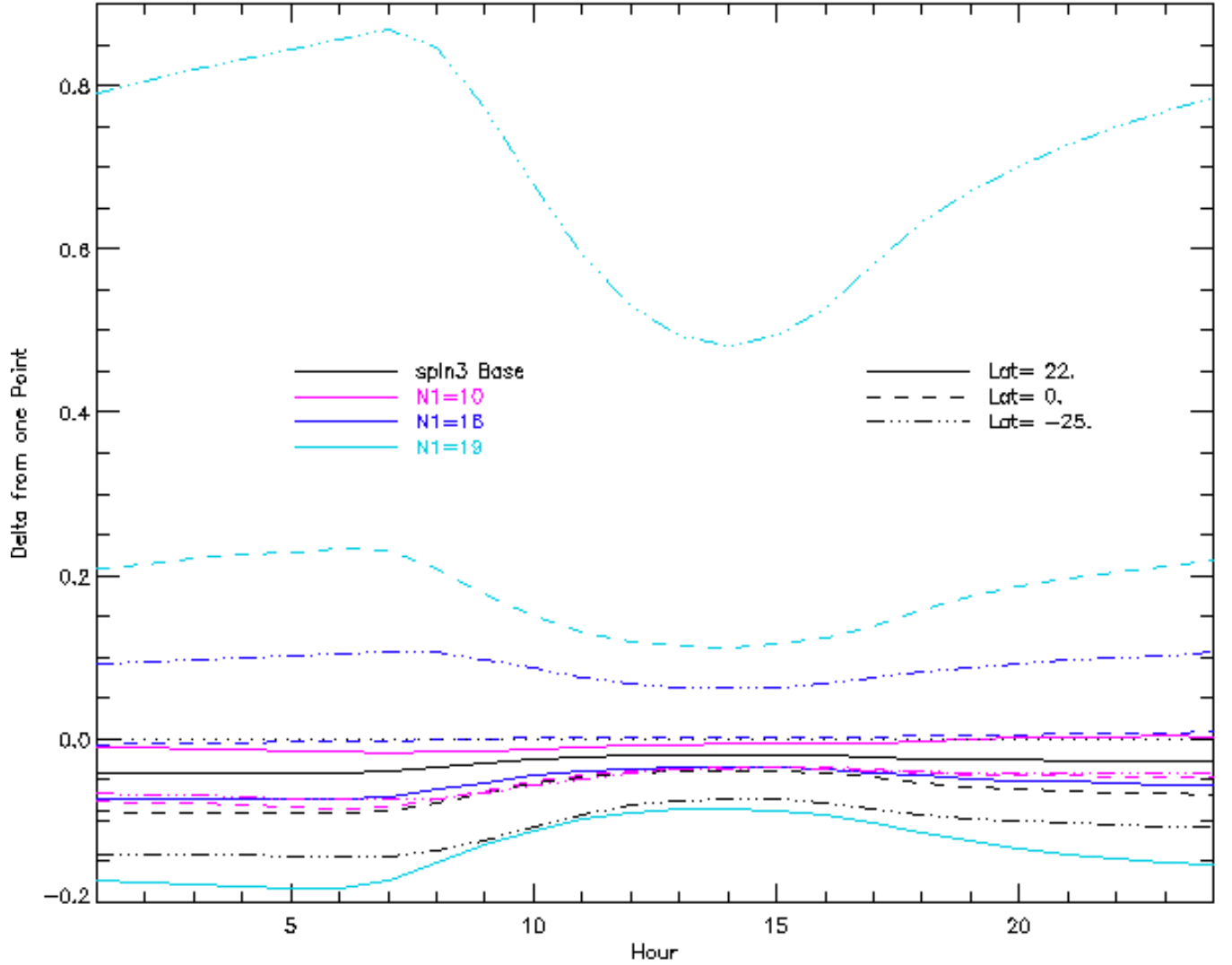


Figure 3: Performance of the One-Point default parameters. Difference in surface temperature of a model with 3-year spinup with date-steps of 1/40'th Mars year before the final year ending at the  $L_s = 100^\circ$ , relative to a One-Point run for  $L_s = 100^\circ$ , for three latitudes. The 4-year runs had 10,13,16 and 19 layers, corresponding the bottom depths of 4.5,8.5,15.6 and 27.7 diurnal skin depths. Differences are generally less than 0.2 K except for the deepest model, with a total thickness greater than an annual skin depth, at a winter latitude when memory of the annual average temperature warms the surface, especially at night.



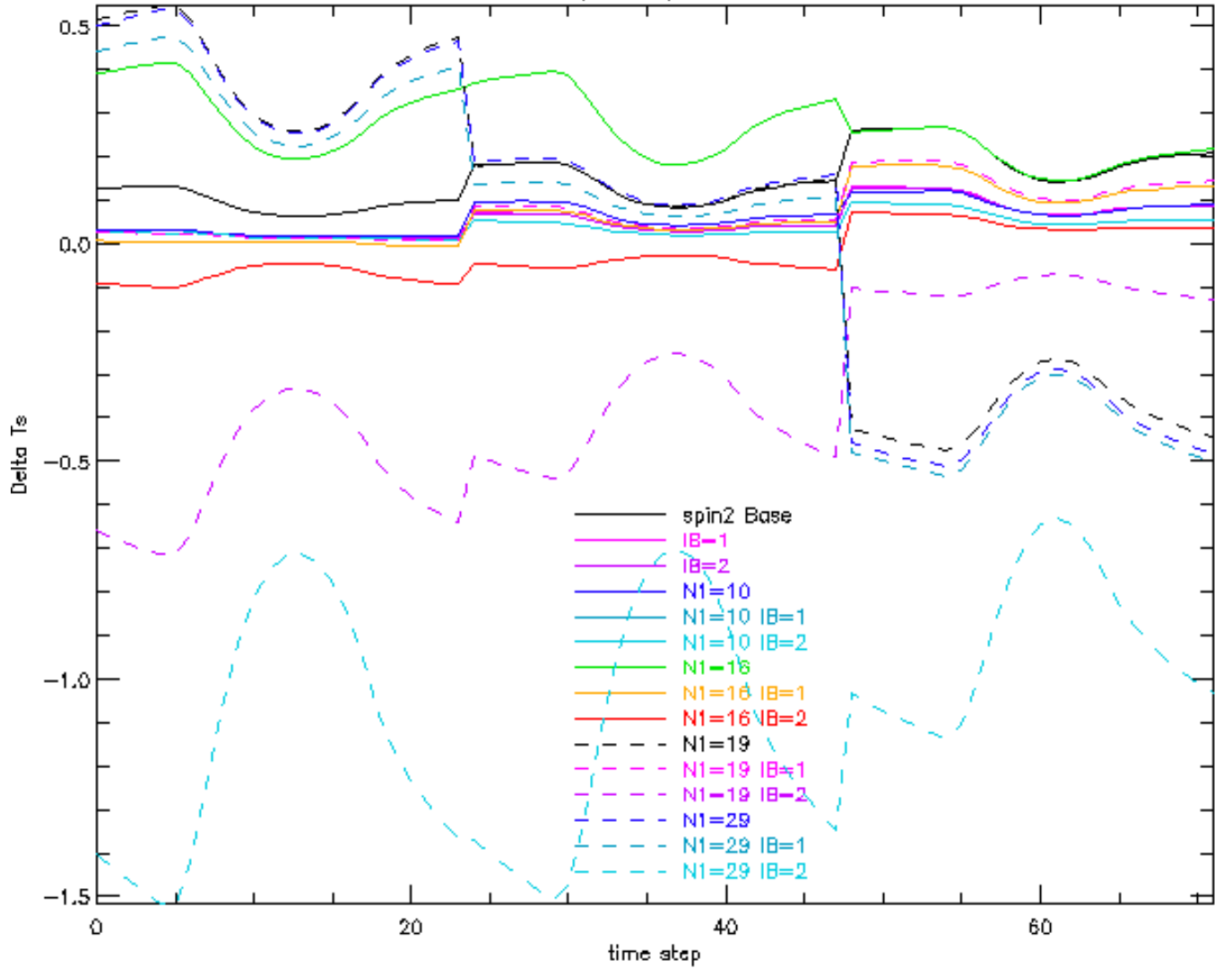


Figure 4: Difference in  $T_s$  between 20 sol and 3 year spinup for three latitudes at  $L_s = 100^\circ$ . The left one-third of the plot shows diurnal results at 22 N, the middle third at 0 N, and the right at 25 S; the lines connecting these sections are non-physical but assist in following the same case. Cases that are not apparent are covered by the lines of the next case; e.g., N1=10 IB=1 is obscured by N1=10 IB=2.

## 3.4 Comparison to other thermal models

### 3.4.1 Comparison to Ames GCM

As a check on atmosphere temperatures and down-going radiance, a specific test case was chosen for comparison of the KRC one-layer atmosphere with the multi-layer radiative, conductive and convective-coupled atmosphere of a full Global Circulation Model (GCM), [31]; the Viking-1 landing site, Latitude  $22^\circ\text{N}$ , elevation  $-3.1\text{ km}$ ,  $L_s = 100^\circ$ ,  $\tau = 0.3$ , visible/IR opacity ratio 1.0, surface pressure of 7 millibar, bolometric albedo of 0.25, thermal inertia  $270\text{ J m}^{-2}\text{s}^{-1/2}\text{K}^{-1}$ , soil density =  $1600\text{ kg/m}^3$ , soil specific heat =  $630\text{ J/kg}$ , model depth =  $40\text{ m}$ . This special GCM run inhibited lateral atmospheric dynamics and output a mass-weighted atmosphere temperature; it started with an isothermal profile at  $180\text{K}$  and was “spun up” for 20 sols before the output date (data kindly provided by Robert Haberle).

The resulting temperatures and fluxes are shown in Figure 5, along with those for three KRC runs. The KRC base model used the parameters shown in Appendix A, apart from the values listed above, use of 29 layer, and the bottom at 8 m is held at  $180\text{ K}$  to approximate the effect of the deeper GCM sub-surface; the diurnal skin-depth is  $45\text{ mm}$ .

The KRC and GCM atmospheric temperatures have similar mean, variation, and phase, with minima near 8H and maxima near 17H; however, the KRC down-going infrared radiance lags the GCM slightly, as expected because the GCM near-surface atmospheric layers dominate the down-going flux and they track the surface temperature more closely than the KRC one-layer atmosphere.

The KRC atmosphere down-going infrared radiances are similar in diurnal behavior but larger than the GCM; use of the KRC default value of 0.5 for ID/solar opacity ratio results in values closer to the GCM, with modest changes in  $T_s$  and  $T_a$  (lower set of curves in Figure 5) .

The GCM surface temperatures are lower than base KRC model by 5-9, due in part to initializing all layers at a temperature about  $40\text{K}$  below the surface average. A KRC model with realistic deep temperatures has  $T_s$  and  $T_a$  a few degrees higher and 5% higher IR flux (upper set of curves in Figure 5).

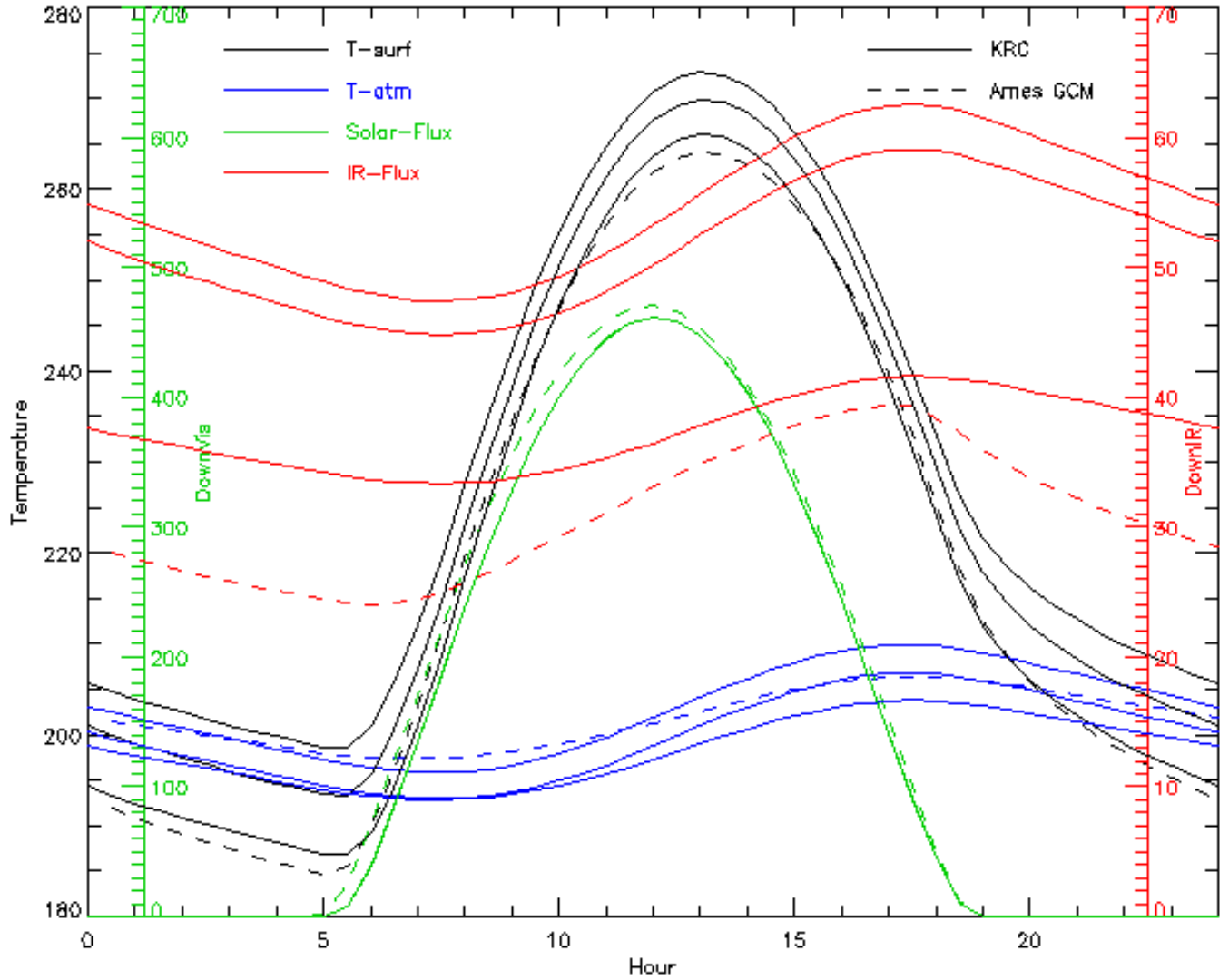


Figure 5: Comparison with Ames GCM results. Calculations for the Viking Lander 1 site at  $L_s = 100^\circ$  for albedo=0.25,  $TI=270$ ,  $\tau = 0.3$  and  $\tau_{IR}/\tau_{Vis} = 1.0$ . The surface kinetic temperature [black]; mass-weighted temperature of the atmosphere [blue], down-going infrared radiation at the surface (red, right auxiliary axis), and down-going total insolation at the surface (green, left auxiliary axis). Three KRC runs are shown: the middle for each parameter is with the same input values as the GCM; the lower has  $\tau_{IR}/\tau_{Vis} = 0.5$ , the KRC default; and the upper starts with equilibrium temperatures and allows the bottom temperature to jump to prevent net heat flow.

### 3.4.2 Comparison to Mellon model

For TES standard processing, Mellon models were generated at 8 sol intervals and  $5^\circ$  latitude spacing for 10 thermal inertia's spaced logarithmically; for 3 sets of albedo, 3 sets of dust opacity, and 3 sets of average surface pressure. Mellon uses a multi-layer radiative-convective atmosphere [42] and his model takes about two orders of magnitude longer to run than KRC (Mellon, personal communication). KRC models were generated on the same grid, except only latitudes 85, 60, 30 and 0, both N and S and for the middle value of albedo (0.25), dust opacity (0.5), and average surface pressure (600 Pa). The same values were used for all physical parameters identified in the Mellon model file headers. Mellon models were two years before the output year [42] and KRC 3 years before the output year. The diurnal surface temperature curves for three thermal inertias and three latitudes are shown in Figure 6. KRC models are a few degrees warmer, the greatest at night and for low thermal inertia. A seasonal comparison is shown in Figure 7; the models track each other closely except for the lowest inertia at 30S near  $L_s = 90^\circ$ , when  $\text{CO}_2$  frost forms at night in only the Mellon model. Mellon midday temperatures are generally slightly higher than KRC at midday and 0 to 4 K cooler predawn. Differences are largest for the lowest thermal inertia and have smooth variation with season unless  $\text{CO}_2$  frost forms.

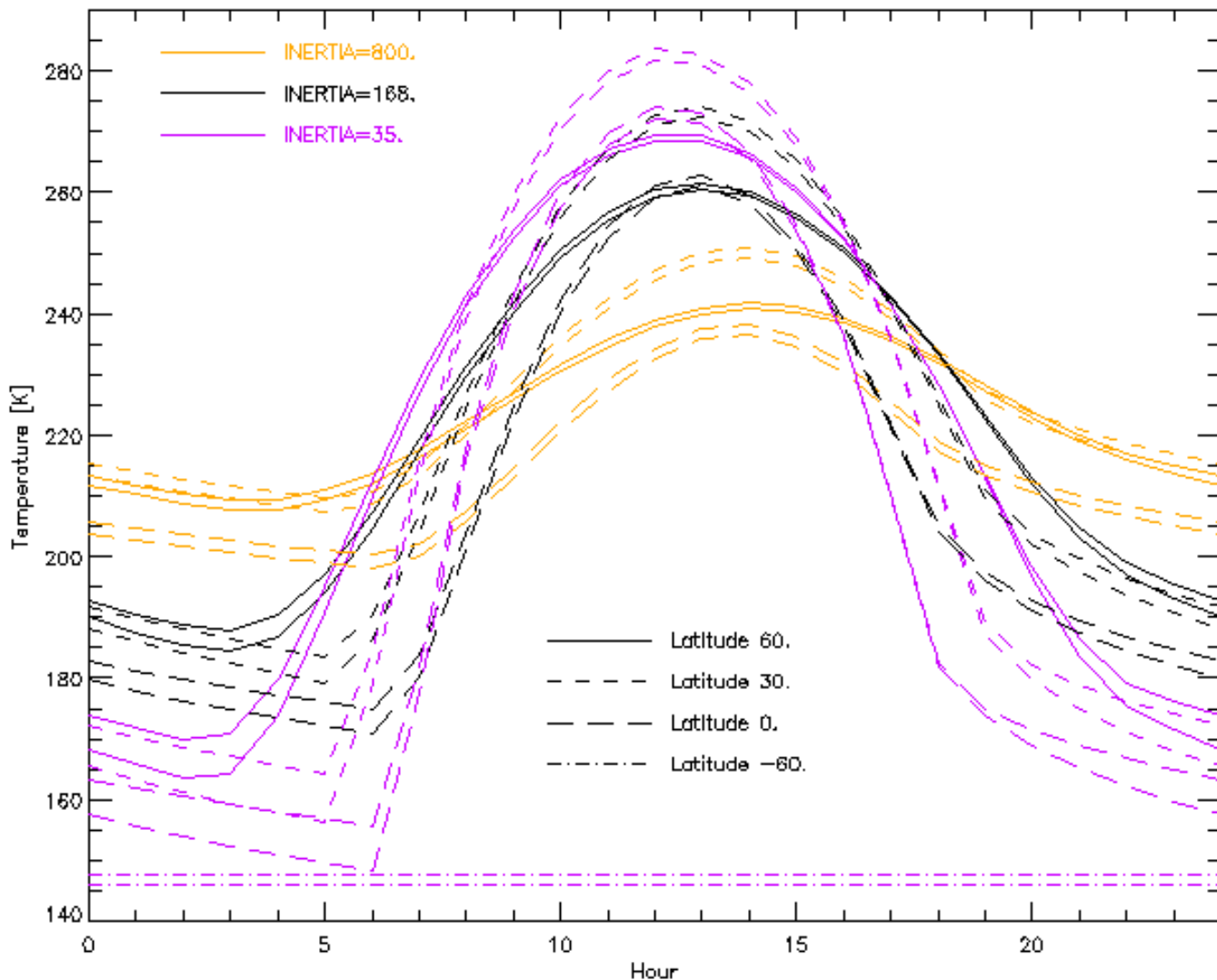


Figure 6: Comparison of KRC with the Mellon models used for TES standard production;  $T_s$  surface kinetic temperature. Diurnal curves for TI of 35 [orange], 168 [black] and 800 [purple] for latitudes 60S, 0, 30N and 60N, all at  $L_s = 100^\circ$ . Both models had seasonal frost all day long at 60S. KRC models are a few degrees warmer, the greatest at night and for low thermal inertia.

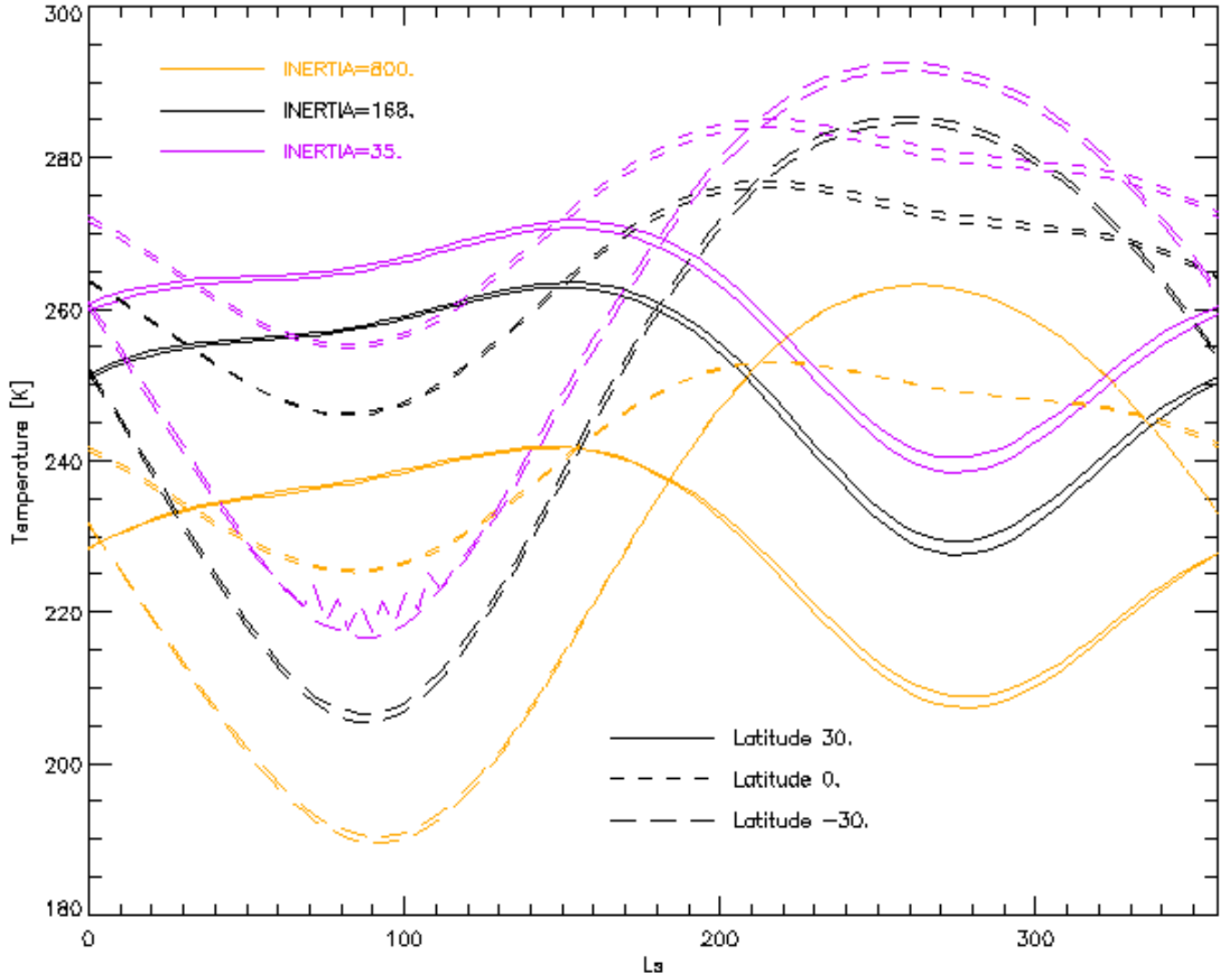


Figure 7: Comparison of KRC with the Mellon models used for TES standard production;  $T_p$  planetary bolometric temperature. Seasonal curves for TI of 35, 168 and 800 for latitudes 30S, 0 and 30N, all at 13H. The models track each other closely except for the lowest inertia at 30S near  $L_s = 90^\circ$ , when  $\text{CO}_2$  frost forms on some nights in the KRC models. Mellon midday temperatures are slightly higher than KRC except for  $I=800$  at Latitudes 0 and 30 N near  $L_s = 90^\circ$

### 3.4.3 Comparison to Vasavada model

Ashwin Vasavada has developed a model used at JPL for martian surface environments. It incorporates temperature-dependent heat capacity and has the ability to model sloped surfaces. The subsurface portion is based on [67] and the atmosphere interaction is based on a 1-D version of the radiative transfer and boundary layer physics from the GFDL Mars GCM, circa 2004 [71, 56, 9] and includes basic  $\text{CO}_2$  condensation. There is no geothermal heat flux.

Vasavada provided his results for Holden Crater, a candidate landing site.  $A=0.13$ ,  $I=350$  (near 200K), the thermal emissivity is 0.98. The model assumes a constant 10 m/s wind for the boundary layer. After a few years of spin-up and equilibration, the model output values at 15 min time-steps for a martian year. Surface kinetic temperature, down-going solar and down-going thermal radiation at one-hour intervals were supplied. Comparisons are shown for two seasons in Figure 8;  $T_s$  and solar flux compare closely. The Vasavada down-going thermal radiation is greater and has greater amplitude than KRC, the phase relation to KRC is similar to the Ames GCM results.

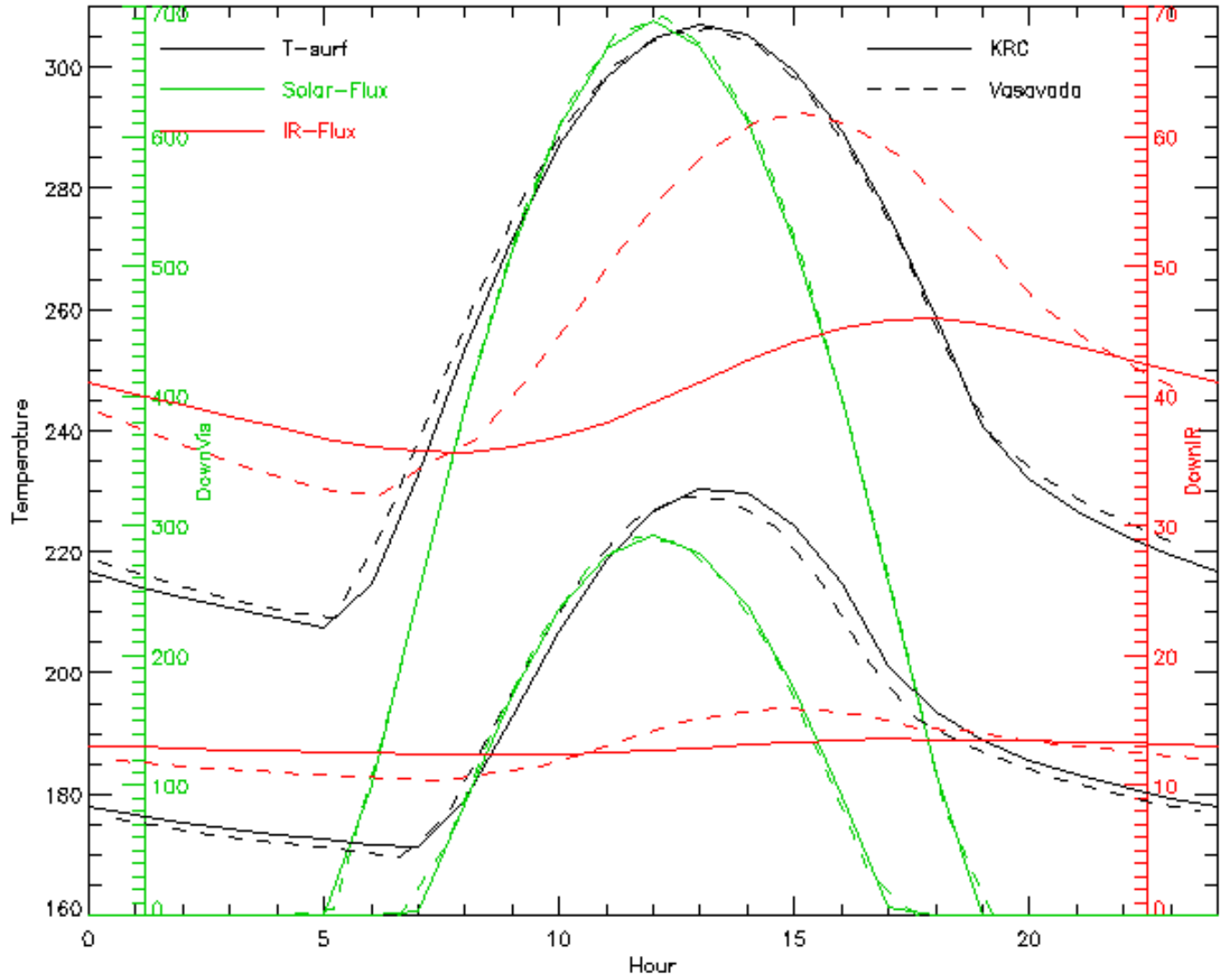


Figure 8: Comparison of KRC (solid lines) with thermal model computed by Ashwin Vasavada (dashed lines). Models are for Holden Crater, a location in the final 4 for MSL; latitude 26.37S, elevation -1.94 km, albedo=0.13,  $I=350$ ,  $\tau_0 = 0.1$ . Two seasons are shown:  $L_s = 91^\circ$  and  $270$ , which correspond to aphelion winter (curves confined to lower half of figure) and perihelion summer (curves rise into upper half of figure). Closely paired curves that do not hit the lower axis are the surface temperature [black], curves hitting bottom are down-going total insolation at the surface [green, left auxilliary axis], central curves are down-going infrared radiation at the surface [red, right auxilliary axis].

## 4 Effect of T-dependent properties

A test of the temperature-dependent code is to invoke it when the properties have no temperature dependence. The effect on  $T_s$  was measured for latitudes 0 and 40S (which has large seasonal variation) over 40 seasons after a 3-year spin-up. For one-material (IC=999) the mean absolute difference was less than 0.3 milli-kelvin, for two-materials (IC=7, 1.6 diurnal skin-depths, 3.5 cm), 0.03 milli-kelvin.

The effect of temperature-dependent materials on surface kinetic temperature was assessed for homogeneous and two-material cases. The base case has  $A=0.25$ ,  $k=0.013$ ,  $\rho=1600$ , and  $C_p=630$  yielding  $I=114.5$ , the lower material has  $k=2.7868$ ,  $\rho=928$ , and  $C_p=1710.65$  yielding  $I=2103.3$ .

For the homogeneous case, and upper material in the layered case, the conductivity is that of sediments in [68] and the specific heat the chlorite of [12]; both scaled slightly to exactly match the above values at  $T=220\text{K}$ . These materials have relatively large T-dependence. The lower material is pure  $\text{H}_2\text{O}$  ice Ih.

For latitude 0, the diurnal behavior is similar all year; the season-averaged results are shown in Figure 9 for temperature-dependent  $K$  and  $C_P$  individually and together. The effects of  $k$ , which generally decreases with temperature, and  $C_P$ , which increases with temperature, somewhat offset each other. The results with a lower layer of ice starting at 1.6 diurnal skin-depths (closer to the surface than generally expected for Mars) are little different from the homogeneous case.

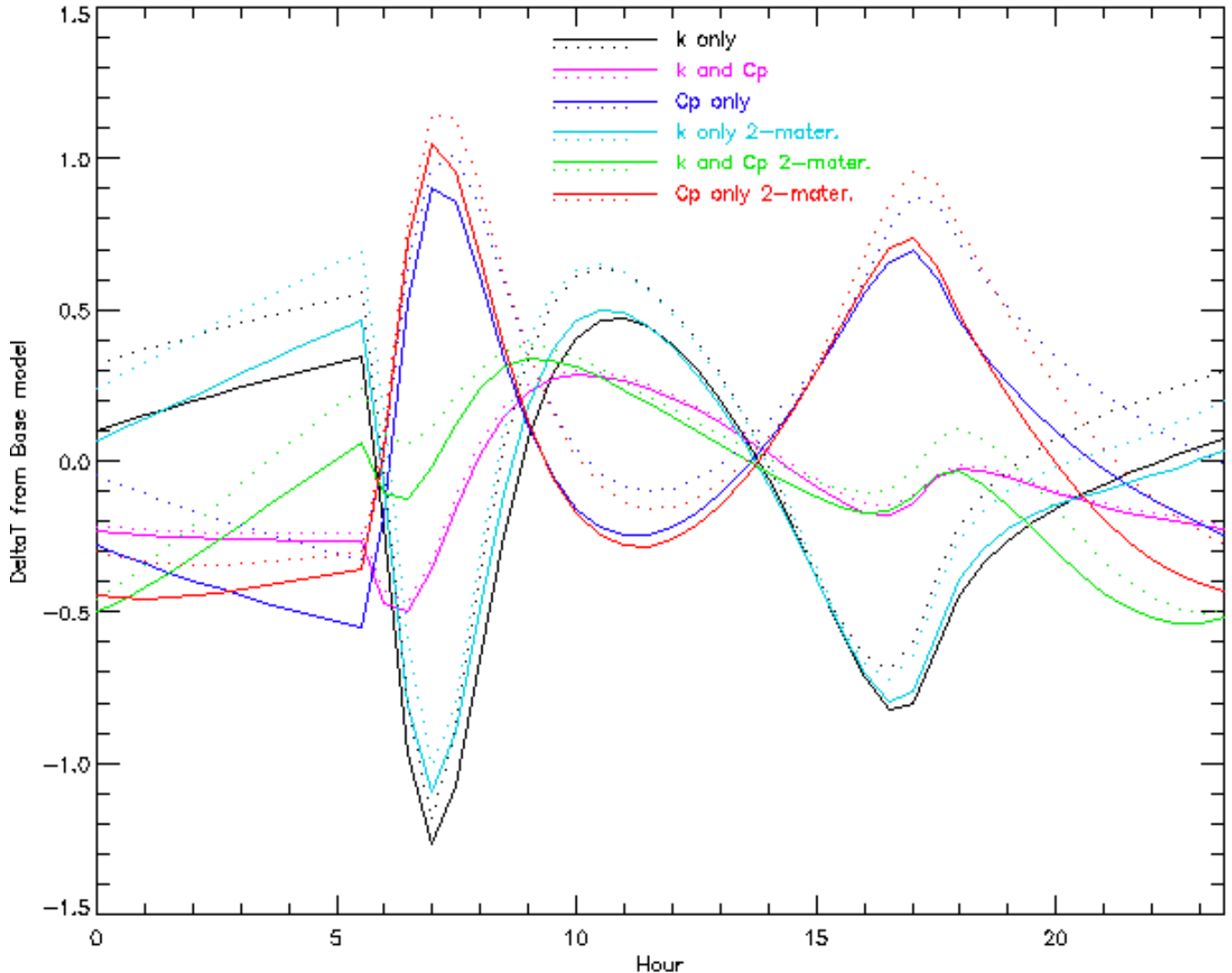


Figure 9: Effect of temperature-dependent thermal properties, shown as the diurnal variation of the surface temperature change for a base case with temperature-independent thermal properties; see the text in §4. Solid lines show the average over 40 uniformly spaced seasons; the dotted lines represent plus one standard deviation. The legend indicates which properties had temperature-dependence for a homogeneous and a two-material case.

## 5 Architecture

The main program can run one or more “cases”, which are normally independent except for retaining the input parameters that are not explicitly changed. However, “linking” runs that transfer forward the current conditions (layer temperatures, frost budget, atmospheric temperature) is possible; see Section 6.1.

The main program, **KRC** calls **TDAY,1** once with a flag that precomputes everything possible about the subsurface numerical scheme, and then for each season calls:

**TSEAS** which loops over seasons, determining the distance and Mars-declination of the Sun, and then calls

**TLATS** which loops over latitudes, calculating insolation and atmospheric parameters for one latitude and calling

**TDAY,2** which does the layer calculations for each time step and each “day” needed to reach convergence.

In addition to the FORTRAN version, IDL interfaces to KRC exist.

## 5.1 Main program, KRC

**KRC** explicitly sets all common areas to zero (not necessary on most modern computers), defines all logical units, sets physical constants, and asks for the input file name and the output log file name. It calls **TCARD,1** to read the input file through complete definition of the first case.

If **TCARD** reports having detected the one-point mode; the 1-point flag is set in common, the initial input file is closed, and the both the file containing the input list of points and the output table file are opened. **TCARD,2** is called to get the first onePoint values.

**KRC** now starts a case and calls **TSEAS**. The remainder of **KRC** is logic and looping control for seasons or onePoints, additional cases, and control of optional printing and binary output files.

## 5.2 Input: TCARD

All input other than the initial two file names is handled by one routine, **TCARD**, which reads lines from the input file[s]. The first integer on a line controls the action to be taken, there are 13 possibilities, described in *helplist.tex*, which allow changing all integer, real, logical input parameters, the latitude set, the elevations set, temperature-dependent properties, titles and file names, and onePoint sets. **TCARD** also tests for formal errors on array sizes, loop limits and some physical constants. A sample input file is shown in Appendix A

## 5.3 Seasons: TSEAS

This routine initializes or increments the season counter and computes the current Modified Julian Date (offset from 2,440,000). If **LSC** true (rare), it calls **TCARD,2** to read any parameter changes and then **TDAY,1** to set up the subsurface model. The Sun-planet geometry is obtained from **PORB** [Planet ORBit] and the  $L_s$  computed; the same geometry is used throughout a “season”. Notification of execution time thus far will be sent to the terminal if **LNOTIF** is True and the season count is a multiple of **NMOD**.

If **SVALB** if True, then at each season the soil albedo will be derived by linear interpolation in  $L_s$  of the albedo table. A similar seasonal variation for atmospheric opacity is available by setting **SVTAU** True.

The routine **TLATS** is called to do calculations for all latitudes, after which there are options to print a diurnal surface temperature table and layer minimum/maximum temperature table by calling the routine **TPRINT**, which handles nearly all printout.

At the end of each season beginning with season count **JDISK**, **TDISK** is called to either write season results as one record in a direct-access binary file (**K4OUT**=0) or save them in one of several formats in a large memory array which is written to a binary file after the last season of the last case.

## 5.4 Latitude calculations: TLATS

**TLATS** is called once per season. Using solar geometry information in Common, it calculates insolation-related values that are constant across latitude. It sets the reference-level surface pressure as described in §2.4.2; if based on polar cap mass, then the routine **TINT** is called to do the global integration of frost amount which in turn controls the global atmospheric pressure. There is an option for **TPRINT,8** to print the global properties.

Looping over latitude, the local surface pressure is calculated. The solar radiation absorbed at the surface and in the atmosphere are calculated for every time-of-day step, including consideration of insolation-dependent frost albedo if that was specified. There is an option to print the values for each hour. The equilibrium temperature conditions are computed; and starting conditions are set to the ending conditions for the prior season, if any.



The routine **TDAY,2** is called to do the diurnal calculations for one latitude. Based on the number of sols required to reach convergence, temperatures at midnight for all layers, the surface, the bottom, and the atmosphere, along with the amount of frost, are predicted to the end of the season; see §3.2.7. There are options to print a convergence summary and hourly radiation conditions.

## 5.5 Diurnal calculations: **TDAY**

The routine **TDAY** continues the inner loops for depth, time of day, and days to convergence; most of the execution time is in this routine. It is coded to minimize the computation time. There are two major sections; **TDAY,1** sets up the subsurface layer and time grid, checking for stability. It computes and saves values that are independent of surface conditions. **TDAY,2** solves the boundary conditions and the diffusion equation, including atmospheric temperature.

**TDAY,2** has an outer loop for days-to-convergence; this resets some summations and for the last day sets the time steps for print and disk output. A middle loop runs over time-of-day; it interpolates the upper two layers to the surface temperature, implements the lower boundary condition, and sets the number of layers to be used for this time step.

There are two inner loops to solve the diffusion equation. For temperature-independent properties they have a total of 10 indexing (2 with fixed offsets) and 6 floating-point operations per layer; if temperature-dependent properties are invoked, these numbers become 17 (3 with offsets) and 33, and involve two subroutine calls. The total execution time is about four times greater for temperature-dependent properties.

After the inner loops, the middle loop finds the new surface heat flow, solves the boundary conditions, computes the new atmospheric temperature and checks for saturation, and modifies any frost amount. If frost appears new or disappears entirely, the frost flag is set appropriately and surface albedo and emissivity reset. If the current day is the last to be computed this season, and the time is on an Hour, then hourly conditions are saved and optionally printed.

In the outer loop, midnight conditions and daily averages are saved. Convergence conditions and iteration counts are checked to see if a jump should be done or if the next day can be the last or if the routine is finished.

## 5.6 Disk Output: **TDISK**

**TDISK** handles all binary input/output. It can write a variety of contents for each season, specified by **K4OUT** as listed in bold at the beginning of items below. These have been developed over time to address various research issues. Planetary temperature is that defined in Eq. 8. The contents of various Commons —**COM** are outlined in §5.7 and detailed in §D.

### 5.6.1 Direct Access files

Direct access files: a record for each season

**-1 KRCCOM** plus **LATCOM**. Only this version supports restarting from a specific season.

**0** One record of **KRCCOM**, latitudes and elevations; then records each season of hourly surface kinetic and planetary brightness temperatures for every latitude. This has been used for most large model sets.

**1 KRCCOM** and **DAYCOM** for the last latitude.

### 5.6.2 Packed binary files

Called “types”, these consist of one multi-dimensional array for all seasons, latitudes and cases, with **KRCCOM** loaded into a “virtual” part of the array. The number of cases that can be accommodated depends upon number of layers, latitudes and seasons and is computed dynamically; more details are in *helplist.tex*, §D.

The memory assigned to store the array is firm coded; the default is adequate for one case of Type 52, with 48 hours, 37 latitudes and 84 seasons. **TDISK** computes the number of cases that it can store for the requested type; if this is less than one, then it will refuse to open an output file.

“Date” is Julian date offset from 2,444,000.

- 51 Surface and planetary temperatures for every hour, latitude and season. Plus, for every season, the date,  $L_s$ , PZREF, dust opacity and total global frost.
- 52 For each latitude; surface, planetary and atmosphere hourly temperature and diurnal layer extremes and NDJ4, DTM4, TTA4, FROST4, AFR04, HEATMM. Plus, for every season, the date,  $L_s$ , PZREF, dust opacity and total frost.
- 54 Surface temperature at 1 and 13 Hours, diurnal-average upward heat flow, midnight frost amount and bottom temperature.
- 55 For one latitude, 10 items related to temperatures, frost and heat-flow. Useful for a large number of seasons.
- 56 Designed for seasonal cap studies; hourly surface and planetary temperatures, plus several parameters at midnight for each latitude, plus several global parameters each season.

## 5.7 Commons

Each common is contained in a separate file that is included into routines at compilation as needed.

**KRCCOM** contains constants that set the sizes of arrays in all commons, all input parameters, most physical constants, and all the major loop indices.

**LATCOM** contains results for latitudes.

**DAYCOM** contains layer temperature extremes and the values at midnight, several conditions at the end of each iteration day, radiation and surface temperature values at each time step, and indices of time-doubling layers.

**HATCOM** contains arrays related to heat flow and irradiance, converged-but-not-predicted atmosphere conditions.

**UNITS** contains logical unit assignments, open/closed flags and error message indices.

**FILCOM** contains all file names

**PORBCM** contains planetary geometry and rotation matrices

## 5.8 Options at compilation

Nearly all size limits are contained in *krccom.inc*

```

PARAMETER (MAXN1 =30)      ! dimension of layers
PARAMETER (MAXN2 =384*4)  ! dimension of times of day: 384=24*16
PARAMETER (MAXN3 =16)    ! dimension of iteration days
PARAMETER (MAXN4 =37)    ! dimension of latitudes
PARAMETER (MAXN5 =161)   ! dimension of saved seasons
PARAMETER (MAXN6 =6)     ! dimension of saved years
PARAMETER (MAXNH =48)    ! dimension of saved times of day
PARAMETER (MAXBOT=6)     ! dimension of time doublings
PARAMETER (KOMMON=1056720) ! Storage for a binary file

```

Size of FFF(KOMMON) in **TDISK** is based on accomodating type 52 for 48 hours, 37 latitudes, and 84 seasons. If one case exceeds KOMMON, **TDISK** will refuse to open an output file.

In *readtxt360.f*, *seasalb.f* and *seastau.f*

```

PARAMETER (MROW=362)      ! max number of table entries

```

## 5.9 Print output

A record of changes and optional notification of season progress appears on the monitor. A separate print file, default name *krc.prt*, is generated for which there are many options, described in the help-list; §D. Voluminous output is possible; it is best to start with the default in the sample input file, §A, then experiment with the options for small cases.

### 5.9.1 Sample layer table

Normally (LP2 true) a layer table is printed at the beginning of each case. This lists the layer thickness and center-depth in both meters and diurnal skin-depth. It also includes the column mass above the center of each layer and the safety factor beyond classical numerical stability. If seasonal memory is not required, then a scaled center depth of order five is adequate. Mars annual skin-depth is 25.85 times the diurnal skin-depth; if the effect of seasonal memory is desired, then the bottom depth should exceed this. An overly deep layer table with sub-surface dirty H<sub>2</sub>O ice follows:

```

Conductiv.= 3.968E-02  Dens*Cp= 1.008E+06  Diffu.= 3.937E-08  Scale= 3.335E-02
Beginning at layer 9  At 0.0931 m.  Inertia= 2025.3
Conductiv.= 3.400E+00  Dens*Cp= 1.206E+06  Diffu.= 2.818E-06  Scale= 2.822E-01
0
  ---THICKNESS---      -----CENTER_DEPTH-----  CONVERGENCE
LAYER   scale  meter   scale  meter  kg/m^2  factor
  1     0.1800  0.0060 -0.0900 -0.0030   0.000   0.000
  2     0.2160  0.0072  0.1080  0.0036  11.527   2.851
  3     0.2592  0.0086  0.3456  0.0115  25.359   2.053
  4     0.3110  0.0104  0.6307  0.0210  41.958   2.956
  5     0.3732  0.0124  0.9729  0.0324  61.877   2.129
  6     0.4479  0.0149  1.3834  0.0461  85.779   3.065
  7     0.5375  0.0179  1.8761  0.0626  114.462  4.414
  8     0.6450  0.0215  2.4673  0.0823  148.882  6.356
  9     6.5486  0.2184  6.0641  0.2023  351.574  4.576
 10     7.8583  0.2621 13.2676  0.4425  594.805  3.295
 11     9.4299  0.3145 21.9117  0.7308  886.681  2.372
 12    11.3159  0.3774 32.2846  1.0768 1236.934  3.416
 13    13.5791  0.4529 44.7322  1.4920 1657.236  4.919
 14    16.2950  0.5435 59.6692  1.9902 2161.599  7.084
 15    19.5539  0.6522 77.5936  2.5880 2766.835 10.200
 16    23.4647  0.7826 99.1030  3.3054 3493.118 14.689
 17    28.1577  0.9392 124.9142  4.1663 4364.658 21.152
 18    33.7892  1.1270 155.8876  5.1994 5410.505 30.459
 19    40.5471  1.3524 193.0558  6.4391 6665.522 43.860
 20    48.6565  1.6229 237.6575  7.9267 8171.542 63.159
 21    58.3878  1.9474 291.1797  9.7119 9978.767 90.949
 22    70.0653  2.3369 355.4062 11.8541 12147.436 130.966
 23    84.0784  2.8043 432.4780 14.4247 14749.839 188.591
 24   100.8941  3.3652 524.9642 17.5094 17872.723 271.571
 25   121.0729  4.0382 635.9477 21.2111 21620.184 391.063
 26   145.2874  4.8459 769.1278 25.6532 26117.137 563.130
 27   174.3449  5.8150 928.9440 30.9836 31513.480 810.907
 28   209.2139  6.9780 1120.7235 37.3801 37989.0941167.707
 29   251.0567  8.3736 1350.8589 45.0560 45759.8281681.498

```

## 6 Use

Users guide available in *helplist.tex*; see supporting material. For normal runs, the user will be prompted for the name of the input file and the names of a print file. All actions are controlled by the input file.

Runs with various options that affect CO<sub>2</sub> condensation are shown in Figure 10. None of the models match the phase of the Viking pressure variation in the northern summer. Using the uniform thermal inertia and frost albedo relation across both seasonal caps is a significant over-simplification for Mars; yet the basic features are captured by the KRC model.

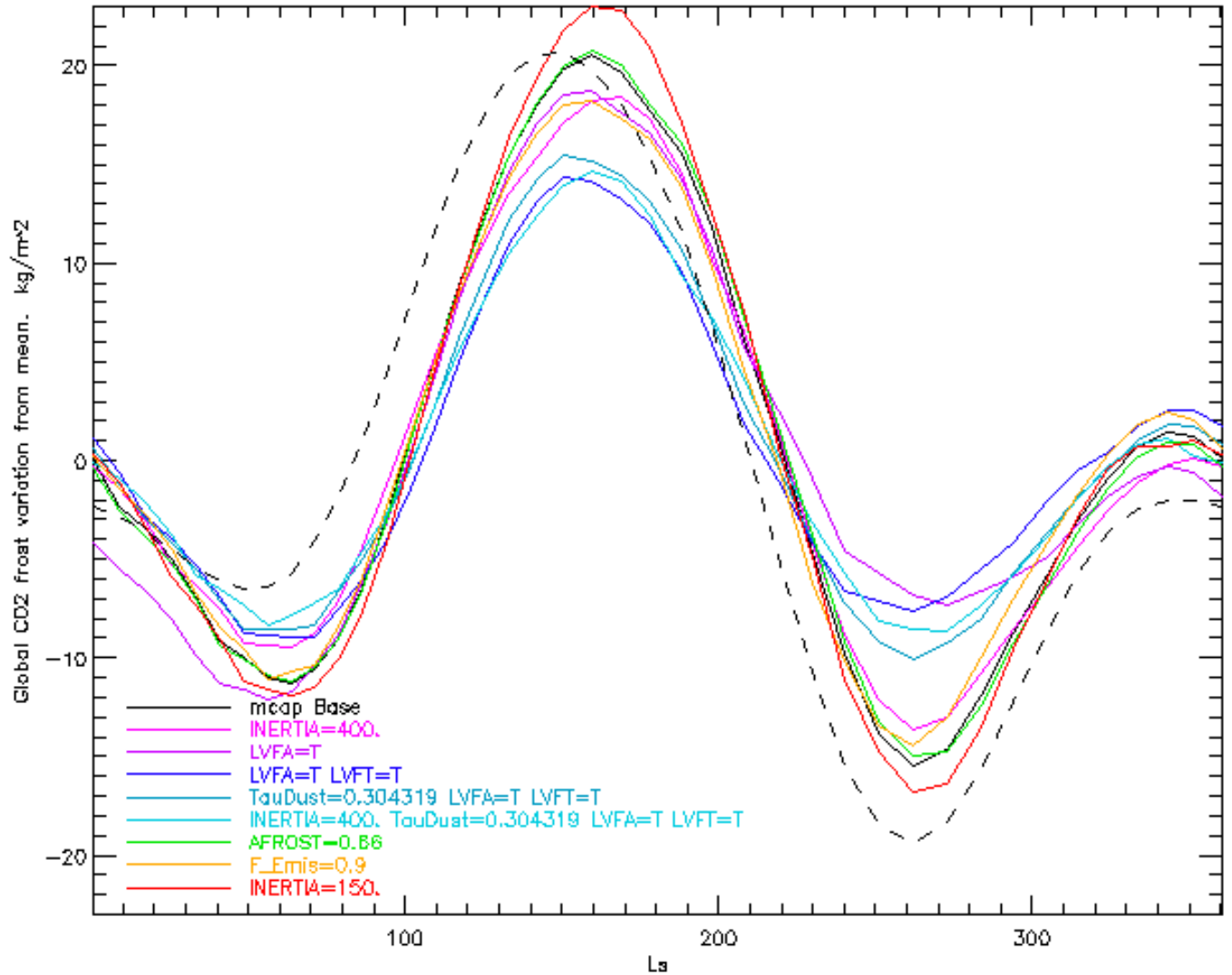


Figure 10: CO<sub>2</sub> frost expressed as changes of global-average column mass in kg/m<sup>2</sup> for nine cases Latitudes at 5° interval, plus ±88.75, with zonal average elevation, 3-year spin-up. Legend lists differences from the base case, which was similar to the default in §A except I=250. LVFA=T means that insolation-dependent frost albedo was used, LVFT=T means that the transition from the albedo of bare ground to that of frost depends upon frost thickness; both these are discussed in §2.4.1. TauDust= means that the seasonal variation of atmospheric opacity of [63] was used. The dashed line shows the mass-equivalent of the pressure variation observed by Viking [64].

## 6.1 Linked Runs

KRC has the ability to continue from the vertical temperature profile at the end of a prior case, as long as the physical distribution of the layers is not changed. It can also start with the conditions at any season in a prior run stored with K4OUT=-1. These can be useful for [at least] two purposes:

- By continuing from memory and incrementing the total number of seasons, it is possible to continuously change parameters in addition to the atmospheric opacity and surface albedo (for which seasonal tables may

be specified).

- Details related to seasonal frost appearance/disappearance. A run-up of a few years with about 40 seasons per year can be used to establish a frost budget and deep temperature profile. Then, the season interval can be set to 1 sol, and events followed in detail.

## 6.2 Routine WHEN2START

If a specific season is desired, an IDL routine is available to compute the proper initial date.

```
function when2start, ls,j5,del
;_Tit1 WHEN2START Calc starting date for KRC to reach Ls on specific season step
; ls   in.   Float.  L_sub_S target
; j5   in.   Integer. Step on which to reach target
; del  in.   Float.  KRC season step size in days OR negative of either:
;                               number of Sols. <35.5 OR intervals per Mars-years >35.5
```

This can be used multiple times for linked runs. For example, to “spin up” for 3 Mars’ years of 40 seasons each, then run daily for 20 sols and end at  $L_s = 100^\circ$ , call in reverse order; because this routine treats indices as 1-based, if second date-interval set adds N intervals, use N+1 as target index.

```
print, when2start(100.,21,1.0275)
    Will print a starting date of 11896.82, at which time  $L_s = 90.86$ 
print, when2start(90.86,120,-40)
    will print the needed starting date of 9853.04
```

## 6.3 One-point version: An alternate input

To support some detailed THEMIS studies, an interface to the KRC system was built that computes the temperature for a single condition. Two input files are involved:

- A “master” file specifying all parameters for a single case. The last line processed must contain the name of the “point” file.
- A “point” file containing formatted lines that each specify the time and conditions at one point; any number of lines are allowed. These values will override those for corresponding items from the master file

The underlying model is the full version of KR and Each point is run as an independent case, so the order of input points is arbitrary.

The default onePoint master file *Mone.inp*, shown in §B.1, has parameters similar to the KRC defaults ( §A ). It specifies one latitude and a layer extending to about 5 diurnal skin depths, so there is virtually no seasonal memory. Thus, it does not treat the seasonal frost properly, and results near the edge of the polar cap are likely to be unreliable. It sets the KRC system into a reasonable mode for one-point calculations with a spin-up of 15 sols. Many parameters in this file could be safely modified.

The fields in the one-point input are:

Ls	$L_S$ season, in degrees
Lat	Aerographic latitude in degrees
Hour	Local time, in 1/24'ths of a Martian Day
Elev	Surface elevation (relative to a mean surface Geoid), in Km
Alb	Bolometric Albedo, dimensionless
Inerti	Thermal Inertia, in SI units
Opac	Atmospheric dust opacity in the Solar wavelength region
Slop	Regional slope, in degrees from horizontal
Azim	Azimuth of the down-slope direction, Degrees East of North.

The two additional columns in the output file are:

TkSur Surface kinetic temperature  
TbPla Planetary bolometric brightness temperature

Execution time is about 3.5 millisecc per point.

## 7 Symbols

Table 1: Symbols and variables

Sym	Name in	Input File label	Value+	Description and basis
-bol	Code	or Equation	frequency	
$A$	AS	ALBEDO	S, $R_f$	Current bolometric albedo.
$B_i$	B		O	Thickness of layer i [m].
$C_p$	SPHT	SpecHeat, SpHeat2	C	Specific heat of the material
$c_p$	ATMCP	Atm_Cp	860. C	Atm. specific heat at constant pressure. $\text{J K}^{-1} \text{kg}^{-1}$ , MARS p.855
$C_1$	CABR	CABR	0.11 C	Clear atmosphere IR absorption.
$C_2$	TAURAT	TAURAT	0.5 C	IR/vis relative opacity. Viking VIS & IRTM opacities. MARS p.1022,3
$F_3$	FAC3	$(1 - A_{[f]})$	S, $R_f$	Surface solar absorbtance.
$F_4$	FAC4	$1 + 1/\text{RLAY}$	O	Layer factor.
$F_5$	FAC5	$\Omega\epsilon\sigma$	O	Surface thermal emission factor.
$4F_5$	FAC45	$4\Omega\epsilon\sigma$	O	Surface thermal emission factor
$F_6$	FAC6	$\Omega\epsilon_{[f]}$	O	Surface emission factor.
$F_7$	FAC7	$\frac{k}{X_2}$	O	Layer scaling.
$F_8$	FAC8	$e^{-\tau_R}\epsilon_{[f]}$	O	Fraction of surface blackbody reaching top-of-atmosphere.
$F_9$	FAC9	$\sigma(1 - e^{-\tau_e})$	O	
$G$	GRAV	GRAV	3.727 C	Martian gravity. $\text{m s}^{-1}$
$G_H$	GO	ARC2	0.5 C	Henyey-Greenstein asymmetry. MARS p.1030
$\mathcal{H}$	SCALEH		S	Scale height in km. Based on TATM*
$H$		$-k\frac{dT}{dz}$		Heat flow
$H_V$	ADGR	S	SR	Solar heating of atm. $\text{Wm}^{-2}$
$i$	I, J			layer index, increaseing downward.
$i$			SR	Incidence angle from zenith onto a horizontal surface.
$i_2$			SR	Incidence angle onto local slope; from SLOPE and SLOAZI
$I$	SKRC	INERTIA		thermal inertia $\equiv \sqrt{k\rho C_p}$
$k$	COND	COND	C	Thermal conductivity of the soil. $\text{Wm}^{-1}\text{K}^{-1}$
$M$			$R_f$	Columnar mass of $\text{CO}_2$ frost $\text{kg m}^{-2}$
$\mathcal{M}$	AMW		43.5 C	Atomic weight of general atmosphere. (g/mole).
$P$	PERSEC	PERIOD [days]		C = diurnal period in seconds
$P_0$	PTOTAL	PTOTAL	689.7 C	Global annual mean surface pressure. Pa
$P_g$	PZREF		S	Current pressure at reference level. Pa
$P$	PRES		S	Current local surface pressure. Pa
$R$	RLAY	RLAY	C	Ratio of thickness of succeeding layers
$R_{\downarrow t}$	ATMRAD	$F_9 T_a^4$	R	Hemispheric emission from a gray slab atmosphere. $\text{Wm}^{-2}$
$S_o$	SOLCON	SOLCON	1368. C	Solar constant. $\text{Wm}^{-2}$
$S_M$	SOL	$S_o/U^2$	S	Solar flux at Mars. $\text{Wm}^{-2}$
$S'_{(t)}$	ASOL		SR	Total insolation onto [sloped] surface. $\text{Wm}^{-2}$
$t$			-	Time ; though a sol from midnight.
$\Delta t$	DTIM			smallest time step
$T$	TSUR		R	Surface kinetic temperature. Kelvin
$T_a$	TATM	TATM	200. C*	Temperature of the atmosphere. Kelvin
$T_a$	TATMJ		R	Temperature of the atmosphere. Kelvin
$T_P$	TPFH		R	Nadir planetary temperature. Kelvin
$U$	DAU	DAU	S	Heliocentric range. Astronomical Units
$W$	POWER		R	Energy into the surface boundary. $\text{Wm}^{-2} \text{s}^{-2}$
$X$	XCEN	XCEN	O	Depth to middle of each layer [m]

Computation frequency (for the temperature-independent properties case) is indicated as:

- C = Input constant
- F = Firm-coded constant
- O = Once
- S = Every “season” (may be as frequent as each sol)
- H = Every “Hour” (24 times per sol)
- R = Rapid: every time-step (Nominal is 384 times per sol)
- SR = every time step for one day each season

subscript  $[f]$  means that frost values are used if frost is present.

‘MARS’ indicates that the values were taken from reference [36] at the listed page.

Table 2: Symbols and variables: Continued

Sym	Name in	Input File label	Value+	Description and basis
-bol	Code	or Equation	frequency	
$\alpha$	1-SKYFAC	$(1 - \alpha)$	S	Fraction of upper hemisphere occupied by ground = slope/180°
$\beta$	BETA	$1 - e^{-\tau_R}$	S	Vertical thermal absorption of atmosphere
$\beta_e$	BETH	$1 - e^{-\tau_e}$	S	Hemispheric thermal absorption of atmosphere
$\gamma$	TWILFAC		S	Twilight extension factor = 90/(90+twilight)
$\delta$	[R]SDEC	SOLARDEC	S	Sub-solar latitude degree [R=radian].
$\epsilon_{[f]}$	EMIS	EMIS	S,R <sub>f</sub>	Surface emissivity. FEMIS for frost
$\theta$	DLAT		S	Latitude. $\theta_2 = \text{latitude} + \text{slope north}$
$\kappa$	DIFFI	$\frac{k}{\rho C_p}$	O	Thermal diffusivity
$\mu_0$	COSI	$\cos i$	SR	Cosine of the incidence angle
$\varpi$	OMEGA	DUSTA	0.9 C	Dust grain single scattering albedo. MARS p.1030
$\rho$	DENS	DENSITY,DENS2	C	bulk density
$\sigma$	SIGSB	5.67051e-8	F	Stephan-Boltzman constant. $\text{W m}^{-2} \text{K}^{-4}$
$\tau_0$	TAUD	TAUD	0.2 C	Nominal solar-range dust opacity
$\tau$	OPACITY		S	Current local dust opacity
$\tau_e$	TAUEFF	Eq. 4	S	Effective thermal opacity of the atmosphere
$\tau_R$	TAUIR		S	Thermal opacity, zenith
$\phi$	ANGLE		R	Hour angle from midnight, $\phi_2 = \text{hour angle} + \text{slope east}$
$\Omega$	SKYFAC	$\equiv 1 - \alpha$	SR	Fraction of the sky (upper hemisphere) that is visible to the surface
$\langle \rangle$				diurnally-averaged value
	TWILI	TWILI	1.0 C	Central angle extension of twilight, degrees
	DTAFAC	$\Delta t / (c_p \frac{P}{g})$	O	Atmosphere heating factor. $\text{s}^2 \text{m}^2 \text{K W}^{-1}$
	FEMIT	$\Omega \epsilon_f \sigma T_f^4$	O	Frost thermal emission.

## References

- [1] R. Arvidson, D. Adams, G. Bonfiglio, P. Christensen, S. Cull, M. Golombek, J. Guinn, E. Guinness, T. Heet, R. Kirk, A. Knudson, M. Malin, M. Mellon, A. McEwen, A. Mushkin, T. Parker, F. Seelos, K. Seelos, P. Smith, D. Spencer, T. Stein, and L. Tamppari. Mars Exploration Program 2007 Phoenix landing site selection and characteristics. *Journal of Geophysical Research (Planets)*, 113(E12):0–+, June 2008.
- [2] R. E. Arvidson, R. C. Anderson, P. Bartlett, J. F. Bell, D. Blaney, P. R. Christensen, P. Chu, L. Crumpler, K. Davis, B. L. Ehlmann, R. Fergason, M. P. Golombek, S. Gorevan, J. A. Grant, R. Greeley, E. A. Guinness, A. F. C. Haldemann, K. Herkenhoff, J. Johnson, G. Landis, R. Li, R. Lindemann, H. McSween, D. W. Ming, T. Myrick, L. Richter, F. P. Seelos, S. W. Squyres, R. J. Sullivan, A. Wang, and J. Wilson. Localization and Physical Properties Experiments Conducted by Spirit at Gusev Crater. *Science*, 305:821–824, August 2004.
- [3] R. E. Arvidson, F. Poulet, R. V. Morris, J.-P. Bibring, J. F. Bell, S. W. Squyres, P. R. Christensen, G. Bellucci, B. Gondet, B. L. Ehlmann, W. H. Farrand, R. L. Fergason, M. Golombek, J. L. Griffes, J. Grotzinger, E. A.



- Guinness, K. E. Herkenhoff, J. R. Johnson, G. Klingelhofer, Y. Langevin, D. Ming, K. Seelos, R. J. Sullivan, J. G. Ward, S. M. Wiseman, and M. Wolff. Nature and origin of the hematite-bearing plains of Terra Meridiani based on analyses of orbital and Mars Exploration rover data sets. *J. Geophys. Res. (Planets)*, 111(E10):12–+, November 2006.
- [4] H. H. Aumann and H. H. Kieffer. Determination of particle sizes in Saturn’s rings from their eclipse cooling and heating curves. *Astron. Jour.*, 183:305–311, 1973.
- [5] J. L. Bandfield. High-resolution subsurface water-ice distributions on Mars. *Nature*, 447:64–67, May 2007.
- [6] J. L. Bandfield and C. S. Edwards. Derivation of martian surface slope characteristics from directional thermal infrared radiometry. *Icarus*, 193:139–157, January 2008.
- [7] J. L. Bandfield and W. C. Feldman. Martian high latitude permafrost depth and surface cover thermal inertia distributions. *J. Geophys. Res. (Planets)*, 113(E12):8001–+, August 2008.
- [8] J. R. Barnes, J. B. Pollack, R. M. Haberle, C. B. Leovy, R. W. Zurek, H. Lee, and J. Schaeffer. Mars atmospheric dynamics as simulated by the NASA AMES General Circulation Model. II - Transient baroclinic eddies. *J. Geophys. Res.*, 98:3125–3148, February 1993.
- [9] S. Basu, M. I. Richardson, and R. J. Wilson. Simulation of the Martian dust cycle with the GFDL Mars GCM. *J. Geophys. Res. (Planets)*, 109(E18):11006–+, November 2004.
- [10] J.F. Bell. *The Martian Surface: Composition, Mineralogy, and Physical Properties*. Cambridge University Press, 2008.
- [11] R. G. Berman and T. H. Brown. Heat capacity of minerals in the system  $\text{Na}_2\text{O}-\text{K}_2\text{O}-\text{CaO}-\text{MgO}-\text{FeO}-\text{Fe}_2\text{O}_3-\text{Al}_2\text{O}_3-\text{SiO}_2-\text{TiO}_2-\text{H}_2\text{O}-\text{CO}_2$ : representation, estimation, and high temperature extrapolation. *Contributions to Mineralogy and Petrology*, 89:168–183, April 1985.
- [12] C. Bertoldi, E. Dachs, and P. Appel. Heat-pulse calorimetry measurements on natural chlorite-group minerals. *American Mineralogist*, 92:553–559, 2007.
- [13] P. R. Christensen, J. L. Bandfield, J. F. Bell, N. Gorelick, V. E. Hamilton, A. Ivanov, B. M. Jakosky, H. H. Kieffer, M. D. Lane, M. C. Malin, T. McConnochie, A. S. McEwen, H. Y. McSween, G. L. Mehall, J. E. Moersch, K. H. Nealon, J. W. Rice, M. I. Richardson, S. W. Ruff, M. D. Smith, T. N. Titus, and M. B. Wyatt. Morphology and composition of the surface of Mars: Mars Odyssey THEMIS results. *Science*, 300:2056–2061, 2003.
- [14] P. R. Christensen, H. Y. McSween, J. L. Bandfield, S. W. Ruff, A. D. Rogers, V. E. Hamilton, N. Gorelick, M. B. Wyatt, B. M. Jakosky, H. H. Kieffer, M. C. Malin, and J. E. Moersch. Evidence for magmatic evolution and diversity on Mars from infrared observations. *Nature*, 436:504–509, July 2005.
- [15] P. R. Christensen, S. W. Ruff, R. Fergason, N. Gorelick, B. M. Jakosky, M. D. Lane, A. S. McEwen, H. Y. McSween, G. L. Mehall, K. Milam, J. E. Moersch, S. M. Pelkey, A. D. Rogers, and M. B. Wyatt. Mars Exploration Rover candidate landing sites as viewed by THEMIS. *Icarus*, 176:12–43, July 2005.
- [16] P. R. Christensen, S. W. Ruff, R. L. Fergason, A. T. Knudson, S. Anwar, R. E. Arvidson, J. L. Bandfield, D. L. Blaney, C. Budney, W. M. Calvin, T. D. Glotch, M. P. Golombek, N. Gorelick, T. G. Graff, V. E. Hamilton, A. Hayes, J. R. Johnson, H. Y. McSween, G. L. Mehall, L. K. Mehall, J. E. Moersch, R. V. Morris, A. D. Rogers, M. D. Smith, S. W. Squyres, M. J. Wolff, and M. B. Wyatt. Initial Results from the Mini-TES Experiment in Gusev Crater from the Spirit Rover. *Science*, 305:837–842, August 2004.
- [17] S. M. Clifford and C. J. Bartels. The Mars Thermal Model (marstherm): a FORTRAN 77 Finite-Difference Program Designed for General Distribution. In *Lunar and Planetary Institute Conference Abstracts*, pages 142–143, March 1986.
- [18] K. S. Edgett and P. R. Christensen. The particle size of Martian aeolian dunes. *J. Geophys. Res.*, 96:22765–+, December 1991.
- [19] W. C. Feldman, M. C. Bourke, R. C. Elphic, S. Maurice, J. Bandfield, T. H. Prettyman, B. Diez, and D. J. Lawrence. Hydrogen content of sand dunes within Olympia Undae. *Icarus*, 196:422–432, August 2008.

- [20] R. L. Fergason, P. R. Christensen, J. F. Bell, M. P. Golombek, K. E. Herkenhoff, and H. H. Kieffer. Physical properties of the Mars Exploration Rover landing sites as inferred from Mini-TES-derived thermal inertia. *Journal of Geophysical Research (Planets)*, 111(E10):2–+, February 2006.
- [21] R. L. Fergason, P. R. Christensen, and H. H. Kieffer. High resolution thermal inertia derived from THEMIS: thermal model and applications. *J. Geophys. Res. (Planets)*, 111:E12004, 2006.
- [22] I. Gatley, H. H. Kieffer, E. Miner, and G. Neugebauer. Infrared observations of Phobos from Mariner 9. *Astrophys. Jour.*, 190:497–503, 1974.
- [23] T. D. Glotch and P. R. Christensen. Geologic and mineralogic mapping of Aram Chaos: Evidence for a water-rich history. *J. Geophys. Res. (Planets)*, 110(E9):9006–+, September 2005.
- [24] M. P. Golombek, R. E. Arvidson, J. F. Bell, P. R. Christensen, J. A. Crisp, L. S. Crumpler, B. L. Ehlmann, R. L. Fergason, J. A. Grant, R. Greeley, A. F. C. Haldemann, D. M. Kass, T. J. Parker, J. T. Schofield, S. W. Squyres, and R. W. Zurek. Assessment of Mars Exploration Rover landing site predictions. *Nature*, 436:44–48, July 2005.
- [25] M. P. Golombek, R. A. Cook, T. Economou, W. M. Folkner, A. F. C. Haldemann, P. H. Kallemeyn, J. M. Knudsen, R. M. Manning, H. J. Moore, T. J. Parker, R. Rieder, J. T. Schofield, P. H. Smith, and R. M. Vaughan. Overview of the Mars Pathfinder Mission and Assessment of Landing Site Predictions. *Science*, 278:1743–+, December 1997.
- [26] M. P. Golombek, R. A. Cook, H. J. Moore, and T. J. Parker. Selection of the Mars Pathfinder landing site. *J. Geophys. Res. (Planets)*, 102:3967–3988, February 1997.
- [27] M. P. Golombek, L. S. Crumpler, J. A. Grant, R. Greeley, N. A. Cabrol, T. J. Parker, J. W. Rice, J. G. Ward, R. E. Arvidson, J. E. Moersch, R. L. Fergason, P. R. Christensen, A. Castaño, R. Castaño, A. F. C. Haldemann, R. Li, J. F. Bell, and S. W. Squyres. Geology of the Gusev cratered plains from the Spirit rover transverse. *J. Geophys. Res. (Planets)*, 111(E10):2–+, January 2006.
- [28] M. P. Golombek, J. A. Grant, T. J. Parker, D. M. Kass, J. A. Crisp, S. W. Squyres, A. F. C. Haldemann, M. Adler, W. J. Lee, N. T. Bridges, R. E. Arvidson, M. H. Carr, R. L. Kirk, P. C. Knocke, R. B. Roncoli, C. M. Weitz, J. T. Schofield, R. W. Zurek, P. R. Christensen, R. L. Fergason, F. S. Anderson, and J. W. Rice. Selection of the Mars Exploration Rover landing sites. *J. Geophys. Res. (Planets)*, 108:8072–+, December 2003.
- [29] R. Greeley, R. E. Arvidson, P. W. Barlett, D. Blaney, N. A. Cabrol, P. R. Christensen, R. L. Fergason, M. P. Golombek, G. A. Landis, M. T. Lemmon, S. M. McLennan, J. N. Maki, T. Michaels, J. E. Moersch, L. D. V. Neakrase, S. C. R. Rafkin, L. Richter, S. W. Squyres, P. A. de Souza, R. J. Sullivan, S. D. Thompson, and P. L. Whelley. Gusev crater: Wind-related features and processes observed by the Mars Exploration Rover Spirit. *J. Geophys. Res. (Planets)*, 111(E10):2–+, January 2006.
- [30] R. M. Haberle and B. M. Jakosky. Atmospheric effects on the remote determination of thermal inertia on Mars. *Icarus*, 90:187–204, 1991.
- [31] R. M. Haberle, J. B. Pollack, J. R. Barnes, R. W. Zurek, C. B. Leovy, J. R. Murphy, H. Lee, and J. Schaeffer. Mars atmospheric dynamics as simulated by the NASA AMES General Circulation Model. I - The zonal-mean circulation. *J. Geophys. Res.*, 98:3093–3123, February 1993.
- [32] J. H. Joseph, W. J. Wiscombe, and J. A. Weinman. The delta-Eddington approximation for radiative flux transfer. *Journal of Atmospheric Sciences*, 33:2452–2459, 1976.
- [33] H. H. Kieffer. Cold jets in the Martian polar caps. *Jour. Geophys. Res., Planets*, 112(E11):8005–+, August 2007.
- [34] H. H. Kieffer. Particulate thermal conduction. TES/THEMIS Team internal memo, 2009. LaTeX document.
- [35] H. H. Kieffer. Temperature dependence of rock thermal properties. TES/THEMIS Team internal memo, 2010. LaTeX document.
- [36] H. H. Kieffer, B. M. Jakosky, C. W. Snyder, and Eds. M. S. Matthews. *Mars*. University of Arizona Press, Tucson, 1992. 1498 pp.

- [37] H. H. Kieffer, T. Z. Martin, A. R. Peterfreund, B. M. Jakosky, E. D. Miner, and F. D. Palluconi. Thermal and albedo mapping of Mars during the Viking primary mission. *J. Geophys. Res.*, 82:4249–4291, 1977.
- [38] H. H. Kieffer, T. N. Titus, K. F. Mullins, and P. Christensen. Mars south polar spring and summer behavior observed by TES: Seasonal cap evolution controlled by frost grain size. *J. Geophys. Res.*, 105(E4):9653–9699, 2000.
- [39] S. W. Kieffer. Thermodynamics and lattice vibrations of minerals. I - Mineral heat capacities and their relationships to simple lattice vibrational models. II - Vibrational characteristics of silicates. III - Lattice dynamics and an approximation for minerals with application to simple substances and framework silicates. *Reviews of Geophysics and Space Physics*, 17:1–59, February 1979.
- [40] M. J. Ledlow, M. Zeilik, J. O. Burns, G. R. Gisler, J.-H. Zhao, and D. N. Baker. Subsurface emissions from Mercury - VLA radio observations at 2 and 6 centimeters. *Astrophys. J.*, 384:640–655, January 1992.
- [41] T. Z. Martin. Thermal correction of MRO CRISM data using photoclinometry and slope-dependent thermal models for the Martian surface. In *Bulletin of the American Astronomical Society*, volume 36 of *Bulletin of the American Astronomical Society*, pages 1160–+, November 2004.
- [42] M. T. Mellon, B. M. Jakosky, H. H. Kieffer, and P. R. Christensen. High-resolution thermal inertia mapping from the Mars Global Surveyor Thermal Emission Spectrometer. *Icarus*, 148:437–455, December 2000.
- [43] S. A. Nowicki and P. R. Christensen. Rock abundance on Mars from the Thermal Emission Spectrometer. *Journal of Geophysical Research (Planets)*, 112(E11):5007–+, May 2007.
- [44] M.M. Osterloo, V.E. Hamilton, J.L. Bandfield, T.D. Glotch, A.M. Baldrige, P.R. Christensen, L.L. Tornabene, and F.S. Anderson. Chloride-bearing materials in the Southern highlands of Mars. *Science*, 319:1651, 2008.
- [45] D. A. Paige. The annual heat balance of the Martian polar caps from Viking observations. *Ph.D. thesis*, California Inst. of Technology., 1985.
- [46] D. A. Paige. The thermal stability of near-surface ground ice on Mars. *Nature*, 356:43–45, 1992.
- [47] D. A. Paige, J. E. Bachman, and K. D. Keegan. Thermal and albedo mapping of the polar regions of Mars using Viking thermal mapper observations 1. north polar region. *J. Geophys. Res.*, 99:25,959–25,991, 1994.
- [48] D. A. Paige and K. D. Keegan. Thermal and albedo mapping of the polar regions of Mars using Viking thermal mapper observations 2. south polar region. *J. Geophys. Res.*, 99:25,993–26,013, 1994.
- [49] D. A. Paige and S. E. Wood. Modeling the Martian seasonal CO<sub>2</sub> cycle. *Icarus*, 99:15–27, 1992.
- [50] S. Piqueux and P. Christensen. A model of thermal conductivity in planetary soils: 1. Theory for unconsolidated soils. *J. Geophys. Res. (Planets)*, 114(E13):9005–+, September 2009.
- [51] S. Piqueux and P.R. Christensen. North and south subice gas flow and venting of the seasonal caps of Mars: A major geomorphological agent. *J. Geophys. Res.*, 113:E06005, 2008.
- [52] S. Piqueux, C.S. Edwards, and P.R. Christensen. Distribution of the ices exposed near the south pole of Mars using Thermal Emission Imaging System (THEMIS) temperature measurements. *J. Geophys. Res.*, 113:E08014, 2008.
- [53] M. A. Presley and P. R. Christensen. Thermal conductivity measurements of particulate materials 2. results. *J. Geophys. Res.*, 102(E3):6551–6566, March 1997.
- [54] N. E. Putzig and M. T. Mellon. Apparent thermal inertia and the surface heterogeneity of Mars. *Icarus*, 191:68–94, 2007.
- [55] N. E. Putzig, M. T. Mellon, K. A. Kretke, and R. E. Arvidson. Global thermal inertia and surface properties of Mars from the MGS mapping mission. *Icarus*, 173:325–341, February 2005.
- [56] M. I. Richardson, R. J. Wilson, and A. V. Rodin. Water ice clouds in the Martian atmosphere: General circulation model experiments with a simple cloud scheme. *J. Geophys. Res. (Planets)*, 107:5064–+, September 2002.

- [57] A. D. Rogers, P. R. Christensen, and J. L. Bandfield. Compositional heterogeneity of the ancient Martian crust: Analysis of Ares Vallis bedrock with THEMIS and TES data. *Journal of Geophysical Research (Planets)*, 110(E9):5010–+, May 2005.
- [58] S. W. Ruff, P. R. Christensen, R. N. Clark, H. H. Kieffer, M. C. Malin, J. L. Bandfield, B. M. Jakosky, M. D. Lane, M. T. Mellon, and M. A. Presley. Mars’ “White Rock” feature lacks evidence of an aqueous origin: Results from Mars Global Surveyor. *Jour. Geophys. Res.*, 106(15):23921–23928, October 2001.
- [59] K. P. Seidelmann, editor. *Explanatory Supplement to the Astronomical Almanac*. University Science Books, Mill Valley, California, 2005.
- [60] P. K. Seidelmann, B. A. Archinal, M. F. A’Hearn, D. P. Cruikshank, J. L. Hilton, H. U. Keller, J. Oberst, J. L. Simon, P. Stooke, D. J. Tholen, and P. C. Thomas. Report of the IAU/IAG Working Group on Cartographic Coordinates and Rotational Elements: 2003. *Celestial Mechanics and Dynamical Astronomy*, 91:203–215, March 2005.
- [61] P. K. Seidelmann, L. E. Doggett, and M. R. Deluccia. Mean elements of the principal planets. *Astron. Jour.*, 79:57–+, January 1974.
- [62] E. P. Shettle and J. A. Weinman. The Transfer of Solar Irradiance Through Inhomogeneous Turbid Atmospheres Evaluated by Eddington’s Approximation. *Journal of Atmospheric Sciences*, 27:1048–1055, October 1970.
- [63] M. D. Smith. Interannual variability in TES atmospheric observations of Mars during 1999-2003. *Icarus*, 167:148–165, January 2004.
- [64] J. E. Tillman, N. C. Johnson, P. Gettorp, and D. B. Percival. The Martian annual atmospheric pressure cycle: years without great dust storms. *J. Geophys. Res.*, 98:10963–10971, 1993.
- [65] T. N. Titus, H. H. Kieffer, and P. N. Christensen. Exposed water ice discovered near the south pole of Mars. *Science*, 299:1048–1051, 2003.
- [66] T. N. Titus, H. H. Kieffer, and K. F. Mullins. Slab ice and snow flurries in the Martian polar night. *J. Geophys. Res.*, 106(E10):23,181–23,196, 2001.
- [67] A. R. Vasavada, D. A. Paige, and S. E. Wood. Near-Surface Temperatures on Mercury and the Moon and the Stability of Polar Ice Deposits. *Icarus*, 141:179–193, October 1999.
- [68] H. Vosteen and R. Schellschmidt. Influence of temperature on thermal conductivity, thermal capacity and thermal diffusivity of different rock types. *Phys. and Chem. of Earth*, 28:499–509, 2003.
- [69] D.W. Waples and J.S. Waples. A review and evaluation evaluation of specific heat capacities of rocks, minerals, and subsurface fluids. part 1: Minerals and nonporous rocks. *Natural Resources Res.*, 13:97–112, June 2004.
- [70] P. R. Weissman and H. H. Kieffer. Thermal modeling of cometary nuclei. *Icarus*, 47:302–311, 1981.
- [71] R. J. Wilson and K. Hamilton. Comprehensive model simulation of thermal tides in the Martian atmosphere. *J. Atm. Sci.*, 53:1290–1326, May 1996.

## A Sample input file for Mars

Below is a typical input file for Mars. All parameter values should be right-aligned with the parameter name above it. The line beginning “08 Sep 29” and the following block of floating-point numbers specifies the planetary spin axis, the orbit, and contains the associated rotation matrices. All lines below that are “change cards” allowing modification of most parameters; each specified by type (the first number; 1=real 2=integer 3=logical, values greater than 3 have special meaning, explained in *helplist.tex*), location within type (the 2’nd number), new value (the 3’rd number) and a comment which will be printed (4’th item). By FORTRAN convention, everything after a “/” is not read, and thus allows notation in this file. A line beginning with a 0 terminates a set of change cards and starts a new KRC “case”. A 2’nd consecutive 0 will terminate the program.

Parameters whose names begin with a “-” (minus sign) are not used. SOLARDEC, DAU and HLON over over-ridden by orbital calculations of the **PROB** system unless LPORB is set False (and the 13 PORB lines are omitted). A full description of parameters is in *helplist.tex*.

It is possible (by setting LSC True) to read change cards at each season; this requires care to not change any dimensions.

0 0 / KOLD: season to start with; KEEP: continue saving data in same disk file  
 Default values for all parameters. 19 latitudes with mean Mars elevations

ALBEDO	EMISS	INERTIA	COND2	DENS2	PERIOD	SpecHeat	DENSITY
.25	1.00	200.0	3.4	928.0	1.0275	630.	1600.
CABR	AMW	[ABRPHA	PTOTAL	FANON	TATM	TDEEP	SpHeat2
0.11	43.5	-0.00	510.0	.055	200.	180.0	1300.
TAUD	DUSTA	TAURAT	TWILI	ACR2	[ARC3	SLOPE	SLOAZI
0.3	.90	0.5	0.0	0.5	-0.00	0.0	90.
TFROST	CFROST	AFROST	FEMIS	AF1	AF2	FROEXT	[FD32
146.0	589944.	.65	0.95	0.54	0.0009	50.	0.0
RLAY	FLAY	CONVF	DEPTH	DRSET	DDT	GGT	DTMAX
1.2000	.1800	2.0000	0.0	0.0	.0020	0.1	0.1
DJUL	DELJUL	SOLARDEC	DAU	LsubS	SOLCON	GRAV	AtmCp
10322.33	17.1745	00.0	1.465	.0	1368.	3.727	735.9
ConUp0	ConUp1	ConUp2	ConUp3	ConLo0	ConLo1	ConLo2	ConLo3
0.013	0.0	0.0	0.0	0.220	0.0	0.0	0.0
SphUp0	SphUp1	SphUp2	SphUp3	SphLo0	SphLo1	SphLo2	SphLo3
630.0	0.0	0.0	0.0	1300.	0.0	0.0	0.0
N1	N2	N3	N4	N5	N24	IB	IC
20	384	15	19	120	24	0	7
NRSET	NMHA	NRUN	JDISK	IDOWN	FlxP14	FlxP15	KPREF
3	24	1	81	0	45	65	1
K4OUT	JBARE	Notif	[IDISK2				end
52	0	20	-0				0

LP1	LP2	LP3	LP4	LP5	LP6	LPGLOB	LVFA	LVFT	LkofT
F	T	F	F	F	F	F	F	F	F
LPORB	LKEY	LSC	spare	LOCAL	Prt76	LPTAVE	Prt78	Prt79	L_ONE
T	F	F	F	T	F	F	F	F	F

Latitudes: in 10F7.2 -----7 -----7 -----7 -----7 -----7 -----7 -----7  
 -87.50 -80.00 -70.00 -60.00 -50.00 -40.00 -30.00 -20.00 -10.00 0.00  
 10.00 20.00 30.00 40.00 50.00 60.00 70.00 80.00 87.50 -0.00

Elevations: in 10F7.2 -----7 -----7 -----7 -----7 -----7 -----7 -----7  
 3.51 2.01 1.39 1.22 0.38 0.48 1.17 1.67 1.26 0.17  
 -0.94 -1.28 -1.99 -2.51 -3.52 -4.08 -4.51 -4.38 -2.57 -0.00

08 Sep 29 10:41:33 =RUNTIME. IPLAN AND TC= 4.0 0.55000  
 4.000000 0.5500000 0.8650615 0.3229325E-01 5.000821  
 0.9340634E-01 1.523671 12882.95 686.9650 0.9229904  
 5.544495 24.62280 0.000000 0.4093198 0.000000  
 0.000000 0.000000 0.000000 6.159676 0.4662921  
 0.4172604E-01 0.6197483 4.381073 0.000000 1.228627  
 0.6619807 0.000000 1.391099 0.1075499 -0.3195100E-01  
 0.2263214 -1.246176 -0.5861457 -0.8611114E-01 0.8908045  
 0.4461527 -0.9063585 0.1158813 -0.4063075 -0.4136413  
 -0.4393618 0.7974096 0.9138050 -0.4049719 -0.3095386E-01  
 0.4054090 0.9140893 0.9184200E-02 0.2457525E-01 -0.2094154E-01  
 0.9994786 -0.3252879 -0.8556869 -0.4024770 0.9456150  
 -0.2943530 -0.1384504 0.7823110E-07 0.4256245 -0.9048999

8 0 0 '/work1/krc/mars/masterA.t52' / Disk file name  
 1 12 540. 'PTOTAL set to yield 7 mb at VL1 @ Ls=100' /  
 1 3 114.4727 'Iner' / to match upper k(T)

```

1 4 0.22 'COND2' / to match lower k(T)
1 35 4. 'CONVF' / push time doubling start deeper
0/
3 10 1 'LkofT' / Temperature-dependant conductivity
0/
0/
0/

```

Below is an example of an elaborate set of change cards that looks in detail at the temperatures through the first 40 sols of ice freshly exposed at the bottom of a conical pit. It uses 3 latitudes and does 5 cases; the first is ice freshly exposed to a full hemisphere of sky, followed by pits with slopes of 45 and 25 degrees, then these two pits with a different initial ice temperature

```

7 7 7 'Pit dug to ice by Phoenix' / New title
8 0 0 './output/phx4.t52' / Disk file name/
1 1 .20 'Albedo'
1 3 2025.3 'Inertia for ice' /
1 7 1300. 'Spec heat' / for ice
1 8 928. 'Density' / for ice
1 15 185. 'TDEEP' /
1 17 0.2 'TAUD'
1 39 .001 'GGT: set to avoid ending early' / set for daily output
1 41 11920.2 'DJUL' / starting date
1 42 1.0275 'DELJUL 1 sol' / set for daily output
2 1 19 'Num Layers' /
2 3 1 'N3: set to run each day' / set for daily output
2 4 3 'N4' / number of latitudes
2 5 40 'N5' / total number of seasons = sols
2 7 2 'IB start all =TDEEP' /
2 12 1 'JDISK start immediately' /
2 17 52 'K4OUT: 6 items' / 2 17 51 'K4OUT: 30 layers' /
4 77 77 'New Latitudes' / Must be N4 of them in 10F7.2
    65.00 70.00 72.00 -10.00 0.00 10.00 25.00 45.00 70.00 22.00
5 77 77 'New Elevations' / Must be N4 of them in 10F7.2
    -3.5 -3.5 -3.5 00.0 00.0 00.0 00.0 00.0 00.0 -3.1
0/
1 24 -400. 'Azimuth. Set flag to indicate a pit' /
1 23 45. 'Slope' / slope of pit wall
0/
1 23 65. 'Slope' /
0/
1 23 45. 'Slope' /
1 15 220. ' TDEEP' /
0/
1 23 65. 'Slope' /
0/
0/
0/

```

## A.1 Example layer table

### Sample layer table

```

RUN-CASE 1- 1    05 Nov 19 16:45:41    PAGE= 3
Conductiv.= 3.400E+00 Dens*Cp= 1.206E+06 Diffu.= 2.818E-06 Scale= 2.822E-01
  ___THICKNESS___  _____CENTER_DEPTH_____ CONVERGENCE
LAYER  scale  meter  scale  meter  kg/m^2  factor
  1    0.1800  0.0508 -0.0900 -0.0254  0.000  0.000
  2    0.2160  0.0610  0.1080  0.0305  56.568  2.851
  3    0.2592  0.0731  0.3456  0.0975  124.450  2.053
  4    0.3110  0.0878  0.6307  0.1780  205.908  2.956
  5    0.3732  0.1053  0.9729  0.2746  303.658  2.129
  6    0.4479  0.1264  1.3834  0.3904  420.958  3.065
  7    0.5375  0.1517  1.8761  0.5295  561.718  2.207
  8    0.6450  0.1820  2.4673  0.6963  730.630  3.178
  9    0.7740  0.2184  3.1768  0.8965  933.324  2.288
 10    0.9288  0.2621  4.0282  1.1368 1176.557  3.295
 11    1.1145  0.3145  5.0498  1.4251 1468.437  2.372
 12    1.3374  0.3774  6.2758  1.7711 1818.693  3.416
 13    1.6049  0.4529  7.7469  2.1863 2239.000  2.460
 14    1.9259  0.5435  9.5123  2.6845 2743.368  3.542
 15    2.3111  0.6522 11.6308  3.2823 3348.610  2.550
 16    2.7733  0.7826 14.1730  3.9997 4074.901  3.672
 17    3.3279  0.9392 17.2236  4.8606 4946.449  5.288
 18    3.9935  1.1270 20.8843  5.8937 5992.308  7.615
 19    4.7922  1.3524 25.2771  7.1334 7247.337 10.965
Bottom layers for time doubling:  2  4  6  8 10 12 14 19

```

## B One-point mode examples

### B.1 One-point Master file

This file defines the default set of parameters for a “one-point” KRC run. The change-line starting with a 10 points to the file containing the points to be run, which will over-ride the name of the current input file so that no more lines will be read from this file.

The values for N4 (a single latitude) and JDISK (no binary output file) must not be changed. The value for DJUL (starting date) will be over-riden by one calculated to yield the requested LS on the final season. All the parameters corresponding to columns in the Points file will be overridden.

```

0 0 / KOLD: season to start with; KEEP: continue saving data in same disk file
One-point Master. Default values for all parameters.

```

ALBEDO	EMISS	INERTIA	COND2	DENS2	PERIOD	SPEC_HEAT	DENSITY
.25	1.00	200.0	3.4	928.0	1.0275	630.	1600.
CABR	AMW	-ABRPHA	PTOTAL	FANON	TATM	TDEEP	SpHeat2
0.11	43.5	-0.00	510.0	.055	200.	180.0	1300.
TAUD	DUSTA	TAURAT	TWILI	ACR2	-ARC3	SLOPE	SLOAZI
0.3	.90	0.5	0.0	0.5	-0.00	0.0	90.
TFROST	CFROST	AFROST	FEMIS	AF1	AF2	FROEXT	FD32
146.0	589944.	.65	0.95	0.54	0.0009	50.	0.0
RLAY	FLAY	CONVF	DEPTH	DRSET	DDT	GGT	DTMAX
1.2000	.1800	2.0000	0.0	0.0	.0020	0.1	0.1
DJUL	DELJUL	SOLARDEC	DAU	HLON	SOLCON	GRAV	Atm_Cp
10322.34	5.1375	00.0	1.465	.0	1368.	3.727	735.9
ConUp0	ConUp1	ConUp2	ConUp3	ConLo0	ConLo1	ConLo2	ConLo3

```

0.013      0.0      0.0      0.0      0.220      0.0      0.0      0.0
SphUp0    SphUp1    SphUp2    SphUp3    SphLo0    SphLo1    SphLo2    SphLo3
630.0     0.0      0.0      0.0      1300.     0.0      0.0      0.0
  N1      N2      N3      N4      N5      N24      IB      IC
  13     384     10      1      3      24      0     999
NRSET     NMHA     NRUN     JDISK     IDOWN     I14     I15     KPREF
  3      24      1      0      -7     45     68      1
K4OUT     JBARE     NMOD     IDISK2
  0      0      5      -0
LP1      LP2      LP3      LP4      LP5      LP6 LPGLOB  LVFA  LVFT  debug
  F      F      F      F      F      F      F      F      F      F
LPORB    LKEY     LSC LNOTIF LOCAL  LD16 LPTAVE  Prt.78 Prt.79 LONE
  T      F      F      T      T      F      F      F      F      F
LATITUDES: in 10F7.2  -----7 -----7 -----7 -----7 -----7 -----7 -----7
  1.00 -80.00 -70.00 -60.00 -50.00 -40.00 -30.00 -20.00 -10.00  0.00
Elevations: in 10F7.2  -----7 -----7 -----7 -----7 -----7 -----7 -----7
  1.00  0.00  0.00  0.00  0.00  0.00  0.00  0.00  0.00  0.00
08 Sep 29 10:41:33 =RUNTIME.  IPLAN AND TC=  4.0 0.55000
  4.000000      0.5500000      0.8650615      0.3229325E-01      5.000821
0.9340634E-01      1.523671      12882.95      686.9650      0.9229904
  5.544495      24.62280      0.000000      0.4093198      0.000000
  0.000000      0.000000      0.000000      6.159676      0.4662921
0.4172604E-01      0.6197483      4.381073      0.000000      1.228627
0.6619807      0.000000      1.391099      0.1075499      -0.3195100E-01
0.2263214      -1.246176      -0.5861457      -0.8611114E-01      0.8908045
0.4461527      -0.9063585      0.1158813      -0.4063075      -0.4136413
-0.4393618      0.7974096      0.9138050      -0.4049719      -0.3095386E-01
0.4054090      0.9140893      0.9184200E-02      0.2457525E-01      -0.2094154E-01
0.9994786      -0.3252879      -0.8556869      -0.4024770      0.9456150
-0.2943530      -0.1384504      0.7823110E-07      0.4256245      -0.9048999
1 1 0.2502 'Albedo' / Example of change to base parameters
10 1 0.1 'one.inp' / Name of one-point input file
Free text on any length may follow the above line

```

## B.2 Example One-point Input file

The first two lines are mandatory. The first line is title/reminder line, and may be modified. Second line is a column-title line and is a guide to alignment; all values must not extend to the right the last character of their title. The second line should not be modified.

Each line thereafter will produce a single output line; there is no limit to their number.

Each following line must start with an '11 '; this is a code that tells the full-up KRC that this is a one-point line. The next 9 fields are read with a fixed format, and each item should be aligned with the last character of the Column title. All items must be present, each line must extend at least to the m in Azim; comments may extend beyond that, but they will not appear in the output file. Be sure to have a ;CR; at the end of the last input line, but no blank lines.

```

Title Line, Text transfered to output. This & next line must be present
11  Ls  Lat Hour Elev Alb Inerti Opac Slop Azim <Align each field
11 100.0 22.3 13.5 -3.1 0.20 100.0 0.30 0.0 12.3 Viking Lander 1
11 100. 22.3 13.5 -3.1 0.20 200.0 0.30 5.0 90. VL1
11 100. 22.3 13.5 -3.1 0.20 200.0 0.30 5.0 180. VL1
11 100. 22.3 13.5 -3.1 0.20 200.0 0.30 5.0 270. VL1
11 0. 47.7 13.5 -3.0 0.20 50.0 0.20 5.0 270. Viking Lander 2
11 90. 47.7 13.5 -3.0 0.20 100.0 0.20 0.0 0. VL2
11 90. 47.7 13.5 -3.0 0.20 200.0 0.20 0.0 0. VL2

```



```

11 90. 47.7 13.5 -3.0 0.20 400.0 0.20 0.0 0. VL2
11 90. 47.7 13.5 -3.0 0.15 200.0 0.20 0.0 0. VL2
11 90. 47.7 13.5 -3.0 0.35 200.0 0.20 0.0 0. VL2
11 90. 47.7 13.5 -3.0 0.20 200.0 0.50 0.0 0. VL2
11 90. 47.7 13.5 -3.0 0.20 200.0 1.00 0.0 0. VL2
11 180. -8.75 13.0 16.5 0.20 100.0 0.20 0.0 0. Summit Arsia Mons
11 251. -8.75 13.0 16.5 0.20 100.0 0.20 0.0 0. Arsia Mons perihelion
11 270. -8.75 13.0 16.5 0.20 100.0 0.20 0.0 0. Arsia Mons midsummer
11 270. -8.75 13.0 16.5 0.20 50.0 0.20 0.0 0. Arsia Mons midsummer
11 300. 88.5 12. -3. .3 250.0 0.20 0 0 Polar cap test

```

### B.3 One-point sample output

The one-point mode echos each input line to the monitor. The output below is the print file generated by using the input files in the prior two sections. Any change lines are printed, including the name of the one-point input file.

All computed output temperatures follow the line beginning "C\_END" and the first blank line

One-point Master. Default values for all parameters.

RUN-CASE 1- 0 11 .

OPARAMETER CHANGES

TYPE LOC VALUE

1 1 0.2502 Albedo ALBEDO <Changed

10 1 0.1000 one.inp

---- Start of one-point mode ----

Title Line, Text transferred to output. This & next line must be present

C_END	Ls	Lat	Hour	Elev	Alb	Inerti	Opac	Slop	Azim	TkSur	TbPla	Comment
11	100.0	22.3	13.50	-3.1	0.20	100.0	0.30	0.0	12.	282.08	266.73	Viking Lander 1
11	100.0	22.3	13.50	-3.1	0.20	200.0	0.30	5.0	90.	275.88	261.37	VL1
11	100.0	22.3	13.50	-3.1	0.20	200.0	0.30	5.0	180.	276.02	261.36	VL1
11	100.0	22.3	13.50	-3.1	0.20	200.0	0.30	5.0	270.	277.24	262.43	VL1
11	0.0	47.7	13.50	-3.0	0.20	50.0	0.20	5.0	270.	261.07	247.62	Viking Lander 2
11	90.0	47.7	13.50	-3.0	0.20	100.0	0.20	0.0	0.	278.06	265.67	VL2
11	90.0	47.7	13.50	-3.0	0.20	200.0	0.20	0.0	0.	273.22	261.36	VL2
11	90.0	47.7	13.50	-3.0	0.20	400.0	0.20	0.0	0.	265.04	254.17	VL2
11	90.0	47.7	13.50	-3.0	0.15	200.0	0.20	0.0	0.	277.38	265.26	VL2
11	90.0	47.7	13.50	-3.0	0.35	200.0	0.20	0.0	0.	259.32	248.37	VL2
11	90.0	47.7	13.50	-3.0	0.20	200.0	0.50	0.0	0.	270.91	253.44	VL2
11	90.0	47.7	13.50	-3.0	0.20	200.0	1.00	0.0	0.	265.84	242.99	VL2
11	180.0	-8.8	13.00	16.5	0.20	100.0	0.20	0.0	0.	297.51	295.35	Summit Arsia Mons
11	251.0	-8.8	13.00	16.5	0.20	100.0	0.20	0.0	0.	305.87	302.95	Arsia Mons periheli
11	270.0	-8.8	13.00	16.5	0.20	100.0	0.20	0.0	0.	304.55	301.66	Arsia Mons midsumme
11	270.0	-8.8	13.00	16.5	0.20	50.0	0.20	0.0	0.	307.87	304.93	Arsia Mons midsumme
11	300.0	88.5	12.00	-3.0	0.30	250.0	0.20	0.0	0.	146.00	143.11	Polar cap test

END OF DATA ON INPUT UNIT

Case 17 DTIME: total, user, system= 0.0710 0.0660 0.0050

END KRC

## C FORTRAN and C Routines

The KRC source code is in FORTRAN except for low-level I/O and utility routines written in C. An extensive set of IDL routines to process output files has been written, but are not described here

Name	Description
	Primary routines
KRC	Planet surface thermal model; top routine, MGS-TES version
TSEAS	Advance one "season" along planets orbit
TLATS	Latitude computations
TDAY	Day and layer computations
	Input / output routines
TCARD	Read input file and changes
TDISK	Save/read results at the end of a season; Version with BINF5
TPRINT	Printed output routine
	Specific task routines
ALBVAR	Compute frost albedo as linear function of insolation
ALSUBS	Convert between $L_s$ and days into a Martian year
AVEDAY	Average daily exposure of surface to sunlight.
CO2PT	CO <sub>2</sub> pressure/temperature relation
DEDING2	Delta-Eddington 2-stream solution for single homogeneous layer
EPRED	Asymptotic Prediction of numerical iteration
TINT	Spherical integrals over globe
VLPRES	Viking lander pressure curves
	Orbit geometry routines
PORB	Computes planetary angles and location for specific time.
PORB0	Planetary orbit. Read pre-computed matrices and do rotation; minimal for KRC
ECCANOM	Iterative solution of Keplers equations for eccentric orbit
ORBIT	Compute radius and coordinates for elliptical orbit
	Utility routines listed in Makefile
Fortran	catime.f datetime.f idarch.f sigma.f vaddsp.f xtreme.f binf5.f white1.f
C	b2b.c r2r.c u_move1.c u_move4.c u_swapn.c primio.c pio_bind.c.c
C	binf5_bind.c b_alloc.c b_c2fstr.c b_f2cstr.c b_free.c
	Other routines
IDLKRC	Interface to IDL. Planet surface thermal model MGS-TES version

## D Help-List

KRC: PLANETARY SURFACE TEMPERATURES

HELPLIST.TXT 2011Aug08

Hugh Kieffer. Original code ~1969, many revisions.

Major changes:

2002jul12-17 Replace atmosphere with Delta-Eddington model, and atmospheric temperature based on solar and IR energy balance.

2008nov-2009feb Add capability for temperature-dependant thermal conductivity and 2010feb temperature-dependant specific heat and revision of KRCCOM.

The evolution of KRC code is contained in `evolve.txt`.

A crude diagram of the call architecture is in `flow.txt`

=====

METHOD

See the LaTeX document for a more detailed description: `tes/krc/jpap.tex`

Program is designed to compute surface and subsurface temperatures for a global set of latitudes at a full set of seasons, with enough depth to capture the annual thermal wave, and to compute seasonal condensation mass. For historic reasons, the code has substantial optimization. There are generalities that allow this code set to be used for any solid body with any spin vector, in any orbit (around any star); this is also the source of some of the complexity.

Method is explicit forward finite differences with exponentially increasing layer thickness and binary time increase with depths where allowed by stability. Depth parameter is scaled to the diurnal thermal skin depth. Initially starts at 18 hours with the mean temperature of a perfect conductor. Second degree perturbation is applied at the end (midnight) of the (third) day; this jumps the mean temperature of all layers and the lower boundary to equal the mean surface temperature.

Boundary condition treatment:

- Perturbation solution of quartic equation at surface for each iteration; temperature gradient assumed uniform in top interval.
- Lower boundary may be insulating or constant-temperature.

Atmospheric Radiation:

KRC uses a one-layer atmosphere that is grey in both the solar and infra-red regions. parametric atmosphere. The default atmospheric parameters are based on estimates of Mars' gas and aerosol properties.

Delta-Eddington model for insolation; direct onto sloped surface and diffuse, with possible twilight extension.

Atmosphere temperature based on Delta-Eddington solar absorption and IR opacity [Pre 2002jul16

First-order treatment of scattering of solar radiation.

Diurnal temperature is modeled as sinusoidal with phase shift.]

Keplerian orbital motion; seasons are at uniform increments of time. Mean orbital elements are pre-calculated for any epoch (all planets and several comets) by the PORB code set.

Units are SI; days for orbital motion. (Revised from cal-cgs, 97july)

Options:

- Different Physical properties below a set layer (IC).
- Regional slope
- Three ways to handle seasonal global pressure variation

Atmosphere condensation:

- Global integral of CO2 frost-gas budget can control surface pressure.
- Allows different surface elevation for each latitude zone.
- Zonal frost saturation temperature tracks local surface pressure.
- Option for cap albedo to depend upon mean daily insolation.

#### CONVERGENCE NOTES

Convergence prediction routine can't jump more than one time constant ( $\tau = X^2/2$ ) for the total thickness. Therefore, if  $X(N1)$  is small, make DDT smaller than usual. If DELJUL is much smaller than  $(X(N1))^2/2$ , then DDT can be as large as 0.3. Otherwise DDT must be about 0 for the prediction routine to work well (it assumes the 3rd derivative to be 0).

#### - - - - - INPUT FILE - - - - -

All parameters for KRC are set by a formatted text file. An example is master.inp, which has default values for a 19 latitude set for a run of three martian years, with the last output to disk. Parameter values are listed below their titles, which are in many cases identical to the code name, and last character of the title is above the last location in the field. Thus, integer values MUST be aligned. Titles with a leading "[" indicate that the value is not used. The recommended procedure is to copy master.inp and edit only the values you wish to change. The number of lines of Latitudes and Elevations must match the value of N4, e.g., 2 lines for N4=11:20, entries beyond the N4 position may be left blank or contain the end of the line. The 13 lines following Elevations are a geometry matrix for Mars orientation and orbit in 2005, and should not be touched; they can be replaced by running PORBMN carefully.

The titles lines are skipped, so that you may put comments there carefully

The first input line is always KOLD,KEEP (I\*), which sets file usage.

These are described near the end of this help file under DISK BINARY FILES.

If and only if there is a third non-zero integer, then will read next card as 6 debug flags, IDB1 to IDB6, which are normally zero

The next (normally second) line is free text where you can outline the purpose of your run.

If KOLD=0, then a full set of input values is read.

Change lines may follow immediately after the geometry matrix (see PARAMETER CHANGES section below). The end of definition of a "case" is indicated by a "0/" line. Two successive "0/" lines ends the run.

Items with numbers inset 2 spaces below are computed, not input.  
The source code for 'krccom.inc' indicates which subroutine sets many of the parameters; as the routine name in lowercase just below the parameter name.

-----  
Type 4 Title (20A4) 80 characters of anything to appear at top of each page.

Type 1 Real parameters (8F10.2) =====

Surface Properties

- 1 ALB Surface albedo
- 2 EMIS Surface emissivity
- 3 SKRC Surface thermal inertia [ $J\ m^{-2}\ s^{-1/2}\ K^{-1}$ ] { cal cm \* 4.184e4}
- 4 COND2 Lower material conductivity (IC>0)
- 5 DENS2 Lower material density (IC>0)
- 6 PERIOD Length of solar day in days (of 86400 seconds)
- 7 SPHT Surface specific heat [ $J/(kg\ K)$ ] {cal/(g K) \* 4184.}
- 8 DENS Surface density [ $kg/m^3$ ] {g/cubic cm. \*10}

-----  
Atmospheric Properties

- 9 CABR Atmospheric infrared back radiation coefficient  
2002jul16 IR opacity of dust-free atmosphere
- 10 AMW Molecular weight of the atmosphere
- 11 [ABRPHA UNUSED [Phase of ABRAMP, degrees relative to midnight]
- 12 PTOTAL Global annual mean surface pressure at 0 elev., Pascal[=.01mb]
- 13 FANON Mass-fraction of mean atmosphere that is non-condensing
- 14 TATM Atm temp for scale-height calculations

- 15 TDEEP Fixed bottom temperature. Used if IB>=1.  
16 SPHT2 Lower material specific heat (IC>0)

-----  
Dust & Slope Properties

- 17 TAUD Mean visible opacity of dust, solar wavelengths
- 18 DUSTA Single scattering albedo of dust
- 19 TAURAT Ratio of thermal to visible opacity of dust
- 20 TWILI Twilight extension angle [deg]
- 21 ARC2 Henyey-Greenstein asymmetry factor  
moon = eclipse start time in local Hours
- 22 [ARC3 NOT USED coeff. for planetary heating  
moon = eclipse duration in seconds 0=no eclipse
- 23 SLOPE Ground slope, degrees dip. Only pit may slope beyond pole.
- 24 SLOAZI Slope azimuth, degrees east from north. <-360 is a pit

-----  
Frost Properties

- 25 TFROST Minimum Frost saturation temperature  
may be overridden by local saturation temperature (LVFT)
- 26 CFROST Frost latent heat [ $J/kg$ ] {cal/gm\*4184. [ Not used if
- 27 AFROST Frost albedo, may be overridden (LVFA) [ TFROST never
- 28 FEMIS Frost emissivity [ reached
- 29 AF1 constant term in linear relation of albedo to solar flux
- 30 AF2 linear term in relation of albedo to solar flux units=1/flux  
Aprost = AF1 + AF2 \* <cos incidence> SOLCON / DAU<sup>2</sup>
- 31 FROEXT Frost required for unity scattering attenuation coeff. [ $kg/m^2$ ]  
the greater of this and 0.01 is always used.
- 32 fd32 UNUSED

-----  
Thermal Solution Parameters

- 33 RLAY Layer thickness ratio

34 FLAY First layer thickness (in skin depths)  
 35 CONVF Safety factor for classical numerical convergence  
 0 for no binary time division of lower layers  
 >0.8 for binary time division. Larger is more conservative  
 36 DEPTH Total model depth (scaled) (overrides FLAY if not 0.)  
 37 DRSET Perturbation factor in jump convergence. If = 0., then  
 all layers reset to same average as surface layer. Else,  
 does quadratic curve between surface and bottom averages  
 38 DDT Convergence limit of temperature RMS 2nd differences  
 39 GGT Surface boundary condition iteration test on temperature  
 40 DTMAX Convergence test: RMS layer T changes in a day

-----  
 Orbit Geometry & Constants

41 DJUL Starting Julian date of run -2440000(N5>0)  
 42 DELJUL Increment between seasons in Julian days (if N5>1)  
 43 SDEC Solar declination in degrees. (if Not LPROB)  
 44 DAU Distance from Sun in astronomical units (if Not LPROB)  
 45 SUBS Aerocentric longitude of Sun, in degrees. For printout  
 only. Computed from date unless N5=0(for printout only)  
 46 SOLCON Solar constant Applied Optics 1977 v.16, p.2693: 1367.9 W/m<sup>2</sup>  
 1366.2 Based on figure in Frohlich, Observations of  
 irradiance variations, Space Sci. Rev.,94,15-24,2000  
 47 GRAV Surface gravity. MKS-units  
 48 AtmCp Specific heat at constant pressure of the atmosphere [J/kg/K]

-----  
 Temperature dependent conductivity. Ignored unless LKOFT set.

49 ConUp0 Constant coef for upper material  
 50 ConUp1 Linear in  $k=c_0+c_1x+c_2x^2+c_3x^3$  where  $x=(T-220)*0.01$   
 51 ConUp2 Quadratic "  
 52 ConUp3 Cubic coeff. "  
 53 ConLo0 Constant coef for lower material  
 54 ConLo1 Linear as for ConUp above  
 55 ConLo2 Quadratic "  
 56 ConLo3 Cubic coeff. "

Temperature dependent specific heat. Ignored unless LKOFT set.

57 SphUp0 Constant coef for upper material  
 58 SphUp1 Linear in  $k=c_0+c_1x+c_2x^2+c_3x^3$  where  $x=(T-220)*0.01$   
 59 SphUp2 Quadratic "  
 60 SphUp3 Cubic coeff. "  
 61 SphLo0 Constant coef for lower material  
 62 SphLo1 Linear as for SphUp above  
 63 SphLo2 Quadratic "  
 64 SphLo3 Cubic coeff. "

-----  
 COMPUTED REAL\*4 VALUE

65 HUGE = 3.3E38 nearly largest REAL\*4 value  
 66 TINY = 2.0E-38 nearly smallest REAL\*4 value  
 67 EXPMIN = 86.80 neg exponent that would almost cause underflow  
 68 fd60(2) Spare  
 69  
 70 RGAS = 8.3145 ideal gas constant (MKS=J/mol/K)  
 71 TATMIN Atmosphere saturation temperature  
 72 PRES Local surface pressure at current season  
 73 OPACITY Solar opacity for current elevation and season  
 74 TAUIR current thermal opacity at the zenith  
 75 TAUEFF effective current thermal opacity

76 TATMJ One-layer atmosphere temperature  
 77 SKYFAC fraction of upper hemisphere that is sky  
 78 TFNOW frost condensation temperature at current latitude  
 79 AFNOW frost albedo at current latitude  
 80 PZREF Current surface pressure at 0 elevation, [Pascal]  
 81 SUMF Global average columnar mass of frost [MKS]  
 82 TEQUIL Equilibrium temperature ( no diurnal variation)  
 83 TBLow Numerical limit (Blowup) temperature  
 84 HOURO Output Hour requested for "one-point" model  
 85 SCALEH Atmospheric scale height  
 86 BETA Atmospheric IR absorption  
 87 DJU5 Current Julian date (offset 2440000 ala PORB convention)  
 88 DAM Half length of daylight in degrees  
 89 EFROST Frost on the ground at current latitude [kg/m<sup>2</sup>] {g/cm<sup>2</sup> \* 10.}  
 90 DLAT Current latitude  
 91 COND Top material Thermal conductivity (for printout only)  
 92 DIFFU Top material Thermal diffusivity (for printout only)  
 93 SCALE Top material Diurnal skin depth (for printout only)  
 94 PI pi  
 95 SIGSB Stephan-Boltzman constant (set in KRC)  
 96 RAD Degrees/radian

Type 2 Integer Parameters (8I10) =====

1 N1 # layers (including fake first layer) (lim MAXN1)  
 2 N2 # 'times' per day (lim MAXN2). Must be an even number,  
 should be a multiple of N24 and NMHA.  
 3 N3 Maximum # days to iterate for solution (lim MAXN3)  
 98sep03 This can be 1, but then must use DELJUL ~= PERIOD  
 If N3 lt 3, first day starts on midnight. else at 18H  
 4 N4 # latitudes (lim MAXN4=19). Global integrations done for N4>8  
 5 N5 # 'seasons' total for this run. If 0, then DAU and SDEC will be  
 used as entered for a single season.  
 6 N24 # 'hours' per day stored, should be divisor of N2 (lim MAXNH)  
 7 IB Bottom control: 0=insulating, 1=constant temperature  
 2=start all layers =TDEEP & constant temperature  
 8 IC First layer (remember that 1 is air) of changed properties.  
 if 3 to N1-2. > N1-2 (e.g., 999) =homogeneous  
 -----  
 9 NRSET # days before reset of lower layers; >N3=no reset  
 10 NMHA # 'hour angles' per day for printout (no limit)  
 11 NRUN Run #; appears in some printout  
 12 JDISK Season count that disk output is to begin. 0=none  
 13 IDOWN Season at which to read change cards  
 14 I14 Index in FD of flexible print  
 15 I15 ""  
 16 KPREF Mean global pressure control. 0=constant  
 1= follows Viking Lander curve 2=reduced by global frost, but  
 then N4 must be >8, and latitudes must be monotonic increasing  
 and must include both polar regions (no warning for your failure)  
 -----  
 17 K4OUT Disk output control: See details in DISK BINARY FILES section  
 Three modes of direct access Fortran files; one case per file.  
 --KRCCOM(once), then TSF & TPF;  
 0=KRCCOM,LATCOM each season  
 1:49=KRCCOM,DAYCOM for the last latitude; each season

Modes of bin5 file for multiple cases

- 51=(Hours, 2 min/max, lat, seasons, cases)
- 52=(hours, 7 items, lat, seasons, cases)
- 54=[many seasons, 5 items,lats, cases]
- 55=[many seasons,9 items, cases]
- 56=[packed T hour and depth, latitude,season,case]

- 18 JBARE J5 season count at end of which to set frost amount to 0. 0=never
- 19 NMOD Spacing of season for notification. minimum of 1
- 20 IDISK2 Last season to disk for which to print notice

-----  
COMPUTED I\*4 VALUES

- 21 KOLD Season index for reading starting conditions
- 22 id22(6) 22 and 23 used as flags for season-variable ALB and TAUD
- 28 NFD Number of real items read in
- 39 NID Number of integer items read in
- 30 NLD Number of logical items read in
- 31 N1M1 Temperature vrs depth printout limit (N1-1)
- 32 NLW Temperature vrs depth printout increment
- 33 JJO Index of starting time of first day
- 34 KKK Total # separately timed layers
- 35 N1PIB N1+IB Used to control reset of lowest layer
- 36 NCASE Count of input parameter sets in one run
- 37 J2 Index of current time of day
- 38 J3 Index of current day of iteration
- 39 J4 Index of current latitude
- 40 J5 Index of current "season"

Type 3 Logical Parameters (10L7) =====

- 1 LP1 Print program description. TPRINT(1)
  - 2 LP2 Print all parameters and change cards (2)
  - 3 LP3 Print hourly conditions on last day (3)
  - 4 LP4 Print daily convergence summary (4)
  - 5 LP5 Print latitude summary (5)
  - 6 LP6 Print TMIN and TMAX versus latitude and layer (6)
  - 7 LPGLOB Print global parameters each season
  - 8 LVFA Use variable frost albedo. Uses AF1 & AF2 (real # 29,30)
  - 9 LVFT Use variable frost temperatures
  - 10 LKOFT Use temperature-dependent conductivity and specific heat
- 
- 11 LPORB Call PORB1 just after full input set
  - 12 LKEY Read change item from terminal after main input set
  - 13 LSC Read change cards from input file at start of each season
  - 14 LNOTIF spare
  - 15 LOCAL Use each layer for scaling depth
  - 16 LD16 Print hourly table to FORT.76 [TLATS]
  - 17 LPTAVE Print <T>-<TSUR> at midnight for each layer [TDAY]
  - 18 LD18 Output to fort.78 [TLATS] insolation and atm.rad.coefficients
  - 19 LD19 Output to fort.79 [TLATS] insolation and atm.rad. arrays
  - 20 LONE (Computed) Set TRUE if KRC is in the "one-point" mode
- 

followed in 'krccom' by:

- [real\*4] TITLE(20) 80-character title
- [real\*4] DAYTIM(5) 20-character run date and time



=====

Latitude(s) (10F7.2) N4 latitudes in degrees, no internal separations.  
Latitudes to be in order; south to north. [[If last latitude is  
.LE. 0, will assume symmetric results for global integrations]]

Elevation(s) (10F7.2) N4 values in Km corresponding to latitudes

Orbital Parameters (LPORB=T) Format identical to that produced by PORB  
program set ASCII file output. So these can be directly pasted with an  
editor. see PORBCM.INC

- - - - -

### PARAMETER CHANGES

Fortran List Directed. Change the values in KRCCOM  
White-separated, a "/" terminates the read and leaves remaining values unchanged  
The 4 items are: Integer Integer Numeric\_value 'Text' / Comment  
1: Type (integer) see table below  
2: Index in array (integer), as listed in table above  
3: New value, numeric, will read as real and convert. 0.=false.  
4: Reason, text string within single quotes  
[ after a / (forward slash) nothing is read, so you can use for comments]

The print file will list each change as read, followed by the title of the  
changed item. It is a good idea to look at this print to be sure you changed  
what you intended.

Type	Meaning	Valid Index
0	End of Current Changes	any
1	Real Parameter	1:NFDR
2	Integer Parameter	1:NIDR
3	Logical Parameter	1:NLDR
4	New Latitude Card(s) Follow	any
5	New Elevation Card(s) Follow	any
6	New Orbital Parm Cards Follow (LPORB Must be True)	any
7	Text becomes new Title	any
8	Text becomes new disk or season-variation file name if index=22, read variable ALBEDO if index=23, read variable TAUD	
9	Complete new set of input follows	any
10	Text becomes new One-Point input file name	
11	This is a set of parameters for "one-point" model For this type, 9 values must appear in a rigid format	
12	Set of 2*4 coefficients for T-dep. conductivity. List-directed IO	
13	Set of 2*4 coefficients for T-dep. specific heat. List-directed IO	

For 12 and 13, 8 white-space-separated coefficients must follow after  
the type on the same line, with no intervening index or text

To start variable albedo, use input card:

8 22 0 'AlbedoFileName' / Variable albedo text file name

Can revert to constant albedo by hokey technique of using a bad name. E.g.,

8 22 0 'badName' / turn variable albedo off

Files of text table of value versus season will be read at the start of a  
run. These will apply to ALL latitudes. See example valb1.tab

Variable Tau done the same way, with 22 being replaced with 23

```
COMMON /LATCOM/  see latcom.inc
COMMON /DAYCOM/  see daycom.inc
```

Because the binding routines to IDL are intolerant of any errors, the items in the above commons have not been changed, Rather, in 2004July, and additional common was added as a "catch-all" for any new items.

```
COMMON /HATCOM/  see hatcom.inc
```

Error Returns:

```
"Parameter error in TDAY(1)" : Convergence factor < .8 classic.
    Instability anticipated.
"UNSTABLE; Layer..... TDAY(1):
```

```
DRSET: 0=>      Reset by delta_average_T for each layer:
                  else: reset by {linear + DRSET*quadratic}*{<surf>-<botm>}
TDAY: LRESET    Reset midnight T's for all but top layer.
LDAY           Last day computations
```

----- Handy things -----

The first "hour" in printout and output arrays is 1/24 (strictly, 1/N24) of a sol after midnight. E.g., the last time is midnight, not the first.

Atmospheric scale height, SCALEH, depends upon physical constants and TATMAVE which (2007nov) is always = TATM, input. and GRAV , input

----- DISK BINARY FILES -----

The routine TDISK is used to read or write direct-access binary files or bin5 files. The first season to write is specified by JDISK, all following seasons will go to the same file. For direct-access files, each file record consists of KRCCOM plus LATCOM or KRCCOM plus DAYCOM.

Disk output is largely controlled by the KRC and TSEAS routines.

- - - Items which control file I/O - - - - -

KOLD & KEEP on first input line

```
KOLD: 0= input card set follows; else=disk record number to start from,
      then will read any change cards.
```

```
If LPORB in old file was True, then there must be a PORB card set
as the set of lines following the KEEP,KOLD line
```

```
KEEP: 0= close disk file after reading seasonal record KOLD;
      >0= value of JJJJJ at which to start saving seasons in same disk
      file [overrides JDISK].
```

To start from a prior seasonal run, need to determine the record corresponding to the desired season;

```
KOLD=J5_target - JDISK(old) ; >0
set KEEP=1, change card J5=number of new seasons, set K4OUT.
```

JDISK sets the first season to save results

N5 sets the last season to run

K4OUT sets the record content:

- Will output first record of KRCCOM,ALAT,ELEV, then records of TSF & TPF
- 0 Will output records of KRCCOM+LATCOM. Usual for large data-base.
- +n<=50 Will output records of KRCCOM+DAYCOM for the last computed latitude.

>50 Will write custom bin5 file at the end of a run, with dimensionality from 3 to 5 (more possible). All 5x outputs allow multiple cases, each with a "prefix" for each case consisting of 4 size integers (converted to Float) followed by KRCCOM; after this may come vectors of parameters versus season. The next-to-last dimension is increased to allow room for the prefix to be embedded in the bin5 array. KRC input items that would change any of the bin5 dimensions are not allowed to change between cases. Each dimension is adjusted to the necessary size. Each case has the same structure; this simplifies coding although some items are then present redundantly. The number of cases allowed is set by the size of case one, and printed as MASE at the end of the first case in the print output. Cases beyond the maximum that can be stored will be executed, but not saved.

The first 4 words of the prefix, and of thus of the bin5 array, are:

- (1)=FLOAT(NWKRC) ! Number of words in KRCCOM
- (2)=FLOAT(IDX) ! 1-based index of dimension with extra values
- (3)=FLOAT(NDX) ! Number of those extra
- (4)=FLOAT(NSOUT) ! [Available of other use]

51=(N24 hours, 2: TSF TPF, N4 lats, NDX+ seasons, cases)

The prefix section contains: sub\_array(seasons,5)(0-based index)

0)=DJU5 1)=SUBS 2)=PZREF 3)=TAUD 4)=SUMF

52=(N24 hours, 7 items, N4 lats, NDX+ seasons, cases)

The 7 items are: 1)=TSF 2)=TPF 3)=TAF 4)=DOWNVIS 5)=DOWNNIR

6) packed with [NDJ4,DTM4,TTA4, followed by TIN(2+

7) packed with [FROST4,AFRO4,HEATMM, followed by TAX(2+

The number of layers for TIN and TAX is the smaller of: the number computed and that fit here.

The prefix is identical to Type 51

54= (seasons, 5 items, NDX +nlat, cases)

Items are (0-based index):

0= TSF=surface temperature at 1 am, 1= TSF at 13 hours,

2= HEATMM=heat flow, 3= FROST4=frost amount,

4= TTB4 = predicted mean bottom temperature

The prefix contains DJU5

55= (seasons,NDX+ items,cases). For seasonal studies at one latitude

ITEMS intended to be recoded as needed. Initial version is 9 items:

[Tsur@ 1am,3am,1pm, spare, Tplan @1am,1pm, Surface heat flow,

frost budget, T\_bottom]

The prefix contains DJU5

Can hold very large number of seasons and cases.

THIS MODE DOES NOT SUPPORT CONTINUATION RUNS

56= [vectors&items, latitudes, NDX+ seasons, cases]

The first dimension is: TSF for all hours, TPF at all hours,  
T4 for all layers at midnight, then FROST4,HEATMM,TTA4  
The prefix is identical to Type 51

Once a disk file is opened, any records written will go into that file until a new filename is specified (Type 8 Change line), which closes the current file. It is best to ensure that output file does not already exist. If the file already exists, new output may be written in same area, even if larger than needed.

To run & save various cases for a single season, set N5 and JDISK to 1.

To extract a detailed day by saving DAYCOM to disk, set JDISK=N5, set a new file name, and set K4OUT to desired latitude index (normally 1):

To run continuously with output every K ((1-3) days, set DELJUL=K\*PERIOD  
This will force prediction terms to near 0.

setting N3=1 will turn off all prediction.  
set GGT large (to avoid iteration for convergence)  
set NRSET=999 (to avoid reset of layers)

To continue run with new parameters (e.g., DELJUL)

3 21 1 'flag set to continue'

Note: changing DELJUL will cause reset of DJUL

Must increase the value of N5: e.g., 2 5 <bigger> 'Increase stopping season'

Reset will not occur because J5 continues incrementing

#### ASCII Output Files

krc.prt General results. Stuff output is controlled by LP1:6 & LPGLOB

fort.76

tlats.f: mimic Mike Mellon ASCII files

```
      if (ld16) then
        write(76,761)subs,dlat,alb,skrc,taud,pres
761    format(/,'      Ls      Lt      A      I      TauD      P'
762    format(f7.2,f9.3,f8.3,f9.3)
        write(76,762)qh,tsfh(i),adgr(j),qs

        do i=1,n24
          j=(i*n2)/n24
          qh=i*qhs
          qs=(1.-alb)*asol(j) ! absorbed insolation
          write(76,762)qh,tsfh(i),adgr(j),qs
        enddo
```

fort.78

tlats.f: for average and maximum:

```
      if (ld18) write(78,*)cosi_(i), t_(i),ADGs(i),ADGP(i)
      if (ld18) write(78,*)j5,j4,sol,ave_a,adgir,c52,beta
```

fort.79

tlats.f: for each time-step

```
      if (ld19) write(79,*)adgr(jj),qa,direct,diffuse
```

col 1 = downgoing thermal radiation  
 col 2 = total insolation reaching surface  
 col 3 = direct fraction of insolation  
 col 4 = diffuse fraction of insolation

----- To run two material types (2000jan23)

Set IC to the first layer to have the lower material properties ( >= 3)  
 Set COND2 to the lower material conductivity  
 Set DENS2 to the lower material density  
 Set SPHT2 to the lower material specific heat  
 If LOCAL is False, then initial setting of all layer thicknesses is based upon the scale of the upper material; if it is set True, the thickness of the lower layers is set by their scale.  
 TDAY no longer allows unstable (thin) layers, and will increase the thickness of the layer IC to satisfy the convergence safety factor FCONV if needed. However, the code to check on convergence was retained.

----- Setting temperature-dependant properties

Basic Flag is L10=LK0FT . If this is true, then the 8 input parameters ConUp0 to ConLo3 must be set to yield thermal conductivity as a function of temperature for the upper and lower materials.  $k=c_0 + c_1x + c_2x^2 + c_3x^3$  where  $x=(T-200.)*0.01$

Correspondingly, the 8 input parameters SphUp0 to SphLo3 must be set for specific heat

One way to generate the coefficients is to run for each of the upper and lower materials the IDL procedure KOFTOP, which can call all of the temperature-dependant routines. KOFTOP allows change of its parameters, including grain radius and pressure, and will print the required parameters ready for input to KRC.

Below are sample coefficients for thermal conductivity based on Sylvain Piqueux's numerical model for un-cemented soils; the fit error is <0.1% over 120-320K. Left column is grain radius in micrometers, then the four normalized coefficients ready for inclusion in a KRC input file, followed by the thermal inertia at 220K for nominal density and specific heat.

R(mu)	c0	c1	c2	c3	Iner
10.	0.008274	0.000735	-0.000376	0.000148	89.8
20.	0.012379	0.001280	-0.000629	0.000250	109.9
50.	0.021485	0.002647	-0.001201	0.000483	144.7
100.	0.032051	0.004528	-0.001874	0.000761	176.8
200.	0.046023	0.007569	-0.002743	0.001129	211.8
500.	0.068387	0.014075	-0.003874	0.001687	258.2
1000.	0.086303	0.021288	-0.004146	0.002099	290.1
2000.	0.103743	0.030909	-0.003141	0.002535	318.0
5000.	0.127172	0.049907	0.002019	0.003469	352.1
10000.	0.149810	0.074734	0.011546	0.004939	382.2
20000.	0.185706	0.119913	0.030938	0.007877	425.5
50000.	0.283361	0.250283	0.089327	0.016714	525.6

-----  
RUNNING THE "ONE-POINT" MODE (2002mar08)

A parameter initialization file `Mone.inp` is provided. It sets the KRC system into a reasonable mode for one-point calculations. Do not change that file unless you have read this entire file.

A line near the end of that file points to a file `'one.inp'` which can contain any number of one-point conditions. `'one.inp'` is intended to be edited to contain the cases you want; however, it must maintain the input format of the sample file.

First Line is any title you wish. It must be present.  
The second line is an alignment guide for the location lines. It must be there.

Each following line must start with an `'11 '`; this is a code that tells the full-up KRC that is a one-point line. The next 9 fields are read with a fixed format, and each item should be aligned with the last character of the Column title. All items must be present, each line must extend at least to the `m` in Azim; comments may extend beyond that, but they will not appear in the output file. Be sure to have a `<CR>` at the end of the last input line.

The fields (after the 11) in the one-point input are:

Ls `L_sub_S` season, in degrees  
Lat Aerographic latitude in degrees  
Hour Local time, in 1/24'ths of a Martian Day  
Elev Surface elevation (relative to a mean surface Geoid), in Km  
Alb Bolometric Albedo, dimensionless  
Inerti Thermal Inertia, in SI units  
Opac Atmospheric dust opacity in the Solar wavelength region  
Slop\_ Regional slope, in degrees from horizontal  
Azim Azimuth of the down-slope direction, Degrees East of North.

The two additional columns in the output file are:

TkSur Surface kinetic temperature  
TbPla Planetary bolometric brightness temperature

Try running the binary file first. If that fails, a Makefile is provided to compile and link the program; simply enter `"make krc"` and pray. If this fails, have your local guru look over the Makefile for local dependancies. Suggestions of making the Makefile more universal are welcome.

To run the program, change to the directory where the program was built, and enter `"krc"`. You should get a prompt:

```
?* Input file name or / for default =  
Mone.inp
```

If the initialization file still has this name and is in the same directory, enter a single `"/"` and `<CR>`. Otherwise, enter the full pathname to the initialization file, with no quotes and no blanks.

A second prompt is for the name of the output file:

```
?* Print file name or / for default =  
krc.prt
```

Again, if this is satisfactory, simply enter `/ <CR>` , else enter the desired

file path-name.

----- Comments on the One-point model.

The initialization file of 2002mar08 is set to compute the temperatures at the season requested without seasonal memory. It uses layers that extend to 5 diurnal skin depths. It does not treat the seasonal frost properly, so don't believe the results near the edge of the polar cap. Execution time on a circa 2001 PC may be the order of 0.01 seconds per case.

The underlying model is the full version of KRC. By modifying the initialization file, you can compute almost anything you might want. If you choose to try this, best to read all of this document.

-----  
Debug options

```
tcard.f:335:    IF (IDB1.NE.0) WRITE(IOSP,*)'TCARD Exit: IRET=',IRET,NFD,ID(1)
tday.f:56: 991 IF (IDB2.GE.5) WRITE(IOSP,*) 'TDAY IQ,J4=',IQ,J4,jjo
tday.f:358:C 993      IF (J.EQ.IDB4) THEN
tday.f:490: 9  IF (IDB2.GE.6) WRITE(IOSP,*) 'TDAYx'
tdisk.f:93: 991 IF (IDB3.NE.0) WRITE(IOSP,*)'TDISKa ',KODE,KREC,NCASE,J5,K4OUT
tdisk.f:425:    IF (IDB3.GE.3) WRITE(IOSP,*)'TDISKc KREC=',KREC,LOPN2,IOD2,I
tdisk.f:432:    IF (IDB3.GE.3) WRITE(IOSP,*)'TDISKx KREC=',KREC
tlats.f:44:    IF (IDB2.NE.0) WRITE(IOSP,*)'TLATSa',N1,N1PIB,N2,N24,J5
tlats.f:369: 9 IF (IDB2.GE.3) WRITE(IOSP,*)'TLATSx',N1,N1PIB,N2,N24,J3
tseas.f:37: 991 IF (IDB1.NE.0) WRITE(IOSP,*)'MSEASa',IQ,IR,J5,LSC,N5,LONE
seastau.f:35:    IF (IDB5.NE.0) THEN print table read
seastau.f:51:    IF (IDB5.GT.1) WRITE(IOSP,*)'SEASTAU',LSUB,OUT
```

-----  
Reading type 5x files

IDL routines do not access files directly unless specifically listed.

DEFINEKRC Define structures in IDL that correspond for Fortran commons

Calls: None == None other than IDL library

Firm code of common definitions. Must be recoded if a Fortran \*.inc changes

READKRCCOM Read a KRCCOM structure from a bin5 file

uses 3-element HOLD array. Returns a structure of krccom

Options to open or close bin5 file or read one case

Calls: DEFINEKRC

Files: bin5

HOLD is: 0]=logical unit 1]=number of words in a case 2]=# cases in the file

MAKEKRCVAL Make string of selected KRC inputs: Key=val

Calls: DEFINEKRC

KRCHANGE Find changes in KRC input values in common KRCCOM

Calls: READKRCCOM MAKEKRCVAL

Reads and stores krccom for first case. For each additional case, makes a list of any changes in the flaot, integer or logical input values.

KRCCOMLAB Print KRC common input items

all items via arguments

Calls: None

KRCLAYER Compute center depth of KRC layers  
all items via arguments  
Calls: None

KRCCOMLAB Print KRC common input items  
all items via arguments  
Calls: None

KRCSIZES Compute array and common sizes for KRC Fortran  
Test procedure to compute array sizes or hours.  
Must recode if any size in \*.inc changes  
Calls: None

-----  
A listing of all Fortran commons can be generated by these Linux commands:  
cd /home/hkieffer/krc/src [replace top part of path with local installation]  
rm allinc.txt  
cat krccom.inc latcom.inc daycom.inc hatcom.inc filcom.inc units.inc porbcm.inc > allinc.txt

=====  
Notes on how some aspects of the code work:

>> New file name:

TCARD reads a card of Type 8, (and index is not 22 or 23)  
it calls TDISK(4,0), which closes current file and sets LOPN2=.FALSE.  
TCARD then moves new file name into common  
KRC checks if current (new) values of N5 and JDISK call for file output;  
with LOPN2=.FALSE., KRC calls CALL TDISK (1,0) to open new file.

>> End of a case and end of a run:

TCARD sets KOUNT=0 at entry; this is incremented for every card except those of  
type 0 ( or less) or type 11 (one-point mode). When type 0 is encountered, if  
KOUNT is positive, does normal check of changes before return with IR=1 to  
indicate start of a new case; if KOUNT is zero, returns with IR=5 and prints  
'END OF DATA ON INPUT UNIT'

>> Setting one-point mode.

This can be done only in the first case, and there is no way to leave the  
one-point mode except to end the run.

TCARD encounters: " 10 \* filename" as change card in the initial case.

sets this as new input file name, then returns with IRET=4  
[Thus, nothing following this change card in initial file is read]  
KRC closes prior input file, opens the new one, and reads past first two lines  
then calls TCARD to read first one-point line and sets LONE=true  
and drops into the top of the "case" loop.

The master one-point should have a single latitude, no binary output file.  
The small number of layers, days to converge, and seasons ignores the seasonal  
effect.

One-point request values are read by TCARD @ 310, which computes starting DJUL

TPRINT does linear interpolation of TOUT, which has N2 points between sol. To get Tp,  
does interpolation of Tp-Ts at the hour points, and adds to interpolated Ts.



>> Starting conditions and date

Initial N5-JDISK sets the size of output files. There could be any number of interior seasons where parameter changes are made; based on successive values of IDOWN.

KRC initially calls TCARD(1

For each case loop, sets IQ=TCARD\_return. If one-point mode, sets IQ=1

TSEAS uses IQ as key. If this is 1, then sets J5=0 and sets DJU5 to season -1. else, increments J5 and increments DJU5 with current DELDUL. This allows use of variable resolution dates. (so J5 never 0 when TCARD(2 called)  
If J5 equals IDISK2, then TSEAS calls TCARD(2 to read changes, and proceeds to next season.

TLATS uses J5 as the key; if it is <= 1, then starts from equilibrium conditions, else uses predictions from prior season

The default is that change cards cause a fresh calculation of starting conditions. Exceptions are when J5=IDOWN>0 at TCARD entry

>> Changing parameters within a seasonal run = Continue from memory.

When J5 reaches IDOWN, TSEAS calls TCARD, which will set IRET=3 before reading the new parameters. May change DELJUL to get finer seasonal resolution, but must NOT change N5

Use: Normal restrictions for what may not change for Type 5x files apply.  
E.g., type 56 must NOT change number of latitudes nor total number of seasons.

Set N5 to be the total number of seasons desired, including those after any number of parameter changes; it must NOT be changed later.

Set IDOWN to the season at the beginning of which wish to (first) change parameters. The next set of changes could include a revised (larger) IDOWN.

>> Use of common PORBCM

Contents are described in porbcm.inc,  
PORBCM is filled by TCARD calling PORB0, which reads the first 60 items in 5G15.7 from the input file and sets the value of PI. KRC references porbcm.inc but does not use it.

TSEAS uses a few items to calculate LsubS;

```
CALL PORB (DJU5,DAU,PEA,PEB,HFA,HFB) ! FIND CURRENT PLANET POSITION
TANOM = ATAN2 (PHOXX(2),PHOXX(1)) ! TRUE ANOMOLY
SUBS = MOD(((TANOM+SLP)*RAD)+360.,360.) ! L-SUB-S IN DEGREES
SLP L-SUB-S AT PERIAPSIS
PHOXX(3) VECTOR FROM FOCUS (SUN) TO PLANET: ORBITAL PLANE COORDINATES
TYEAR uses the value for length of year.
```

>> Lower boundary condition and resetting (jumping) layer temperatures.

At the start of a case, TLATS sets the temperature profile linear with depth in one of three ways:

IB=0: top and bottom at equilibrium temperature

IB=1: top at equilibrium temperature, the bottom at TDEEP

IB=2: top and bottom at TDEEP

The kind of resetting is controlled by IB. In TCARD, if IB>0, then N1PIB=N1+1, else N1PIB=N1. T(N1+1) is not reset in the time calculations. In TDAY, for each time step, the temperature of the lower boundary is set equal to T(N1PIB), which results in either zero heat flow (IB=0) or a constant temperature.

>> Seasonal variation of albedo or opacity

When TCARD encounters a type of 8 and an index of 23(tau) [or 22(albedo)], it transfers the text item into FVTAU (which is in COMMON /FILCOM/) and then calls SEASTAU with an Ls of -999. SEASTAU when called with LSUB LT -90 calls (providing IOD3) READTXT360, which reads file. Maximum number of rows is 360, more will be ignored. first and last entry read are wrapped with +,- 360 to Ls to ensure no interpolation faults later. TCARD set the variable Tau flag, KVTAU, true if table-read was successful, else it is set false.

If KVTAU is set, TSEAS calls SEASTAU at start of each season, resetting TAUD.

>> Cap-dependent pressure

TSEAS: BUF(1)=0. ! flag for TINT to compute areas

IF (N4.GT.8) CALL TINT (FROST4, BUF, SUMF)

Tlats

IF (N4.GT.8) THEN ! use global integrations

PCAP = SUMF\*GRAV ! cap\_frost equivalent surface pressure

KPREF.EQ.2

PZREF = PTOTAL - PCAP

PCO2G = PCO2M -PCAP ! all changes are pure CO2